

REGULATORY INFORMATION DISTRIBUTION SYSTEM (RIDS)

ACCESSION NBR: 8204290285 DOC. DATE: 82/04/23 NOTARIZED: NO DOCKET #
 FACIL: 50-244 Robert Emmet Ginna Nuclear Plant, Unit 1, Rochester G 05000244
 AUTH. NAME AUTHOR AFFILIATION
 MAIER, J.E. Rochester Gas & Electric Corp.
 RECIP. NAME RECIPIENT AFFILIATION
 CRUTCHFIELD, D. Operating Reactors Branch 5

SUBJECT: Forwards results of steam generator tube metallurgical rept.

DISTRIBUTION CODE: ZZZZS COPIES RECEIVED: LTR 1 ENCL 1 SIZE: 55
 TITLE: * * * * * SPECIAL DISTRIBUTION CODE * * * *

NOTES: NRR/DL/SEP 1cy.

05000244

RECIPIENT
ID CODE/NAME

COPIES
LTTR ENCL

RECIPIENT
ID CODE/NAME

COPIES
LTTR ENCL

SEE ATTACHMENT

TOTAL NUMBER OF COPIES REQUIRED: LTTR 40 ENCL 40

1. The first part of the document discusses the importance of maintaining accurate records of all transactions. It emphasizes that proper record-keeping is essential for the transparency and accountability of the organization. This section also outlines the various methods used to collect and analyze data, ensuring that the information is reliable and up-to-date.

2. The second part of the document focuses on the implementation of these practices across different departments. It provides a detailed overview of the current state of affairs, highlighting areas where improvements are needed. The text also includes a list of specific actions that must be taken to address these issues, along with a timeline for completion.

3. The third part of the document discusses the role of leadership in driving these changes. It stresses that without strong leadership, any initiative is likely to fail. This section provides examples of successful leadership practices and offers advice on how to foster a culture of innovation and collaboration within the organization.

4. The final part of the document concludes with a summary of the key findings and a call to action. It reiterates the importance of the measures discussed and encourages all employees to take ownership of their role in the process. The document also includes a list of references and a glossary of terms for clarity.

Subject: Steam generator tube rupture

ORB # 5 BC - 5cys

Reg File - 1

NRC POR-1

LPOR-1

NSIC-1

NTIS-1

I & E-1

NRR/RSB-1

NRR/ICSB-1

NRR/MTEB-1

NRR/CSB-1

NRR/MEB-1

NRR/PTRB-1

NRR/HFEB-1

NRR/OLB-1

IE/EPLB-1

NRR/DL/ORAB-1

NRR/DSI/AEB-1

NRR/OSI/RAB-1

NRR D/DL-1

NRR D/DE-1

NRR D/DHFS-1

IE D/DEP-1

DENTON/CASE-1

Speis, T. -1

Rubenstien -1

Johnston, W. V. -1

Knight, J. R. -1

Houston, R. W. -1

NRR D/DST-1

ACRS-6

Dist per

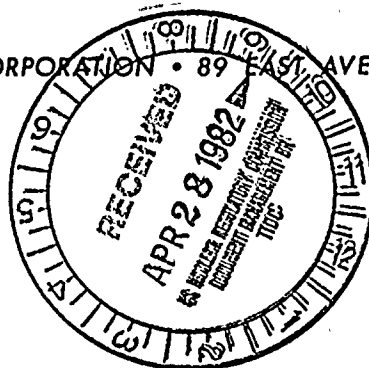
James E. Lyons 4/19/82

Ltr Encl
40 40

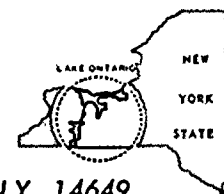


ROCHESTER GAS AND ELECTRIC CORPORATION • 89 EAST AVENUE, ROCHESTER, N.Y. 14649

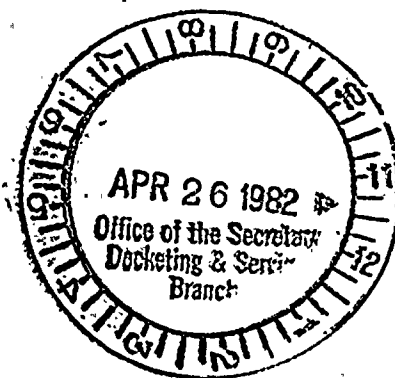
JOHN E. MAIER
Vice President



TELEPHONE
AREA CODE 716 546-2700



April 23, 1982



Director of Nuclear Reactor Regulation
Attention: Mr. Dennis M. Crutchfield, Chief
Operating Reactors Branch No. 5
U.S. Nuclear Regulatory Commission
Washington, D.C. 20555

Subject: Steam Generator Tube Metallurgical Examination
R. E. Ginna Nuclear Power Plant
Docket No. 50-244

Dear Mr. Crutchfield:

By letter dated March 1, 1982, you authorized the removal of a limited number of tube samples from the Ginna B-Steam Generator. These tubes were subsequently removed and sent to our contractor, Westinghouse Electric Corporation for examination. The enclosed report provides the results of that examination. Ten copies of this letter and the enclosed report are provided. Additional copies of the report will be provided in conjunction with submittal of our complete Steam Generator Evaluation report next week.

Very truly yours,

John E. Maier
John E. Maier

Enclosures

2222
s
1/1

8204290285

1000

1000

1000

1000

1000

1000

1000

1000

1000

1000

1000

1000

1000

1000

1000

1000

Metallurgical Examination of Ginna Steam Generator Tubes

Abstract

Detailed microscopic examinations were performed on a section of Row 42 - Column 55 (R42-C55) tubing taken from the hot leg side of the R. E. Ginna "B" steam generator in the region where the tube burst. Five neighboring previously plugged tubes were also examined. All of these Inconel 600 tubes displayed on their O.D. surfaces one or more axially oriented flat zones which contained circumferential striations. Thirty-eight of the forty flat zones that were examined exhibited cold work (O.D.) surface layers, a feature which is consistent with a wear process. The burst in R42-C55 occurred at one of these flats where the wall thickness had been reduced from the nominal 0.050 in. to 0.008 in. Cold work was not identified on the flat that burst. Fractography revealed a normal ductile tensile overload failure at the burst. Fatigue cracking was identified as one mode of breakage of previously plugged tubes. Normal metallurgical properties were identified for the burst tube and for one plugged tube.

1.0 Introduction

On January 25, 1982, a tube ruptured in the "B" nuclear steam generator of the Rochester Gas and Electric Corporation (RGE) R. E. Ginna Power Plant.

The burst tube was determined to be three tube-rows in from the periphery on the hot leg side at Row 42 - Column 55 (R42-C55).

The leak was due to an axially oriented "fish-mouth" opening just above the top of the tubesheet. In addition, some of the previously plugged neighboring peripheral tubes exhibited collapse, deformation, or fracture conditions which were not present at the time these tubes were plugged.

A hole was cut in the shell at Column 55 and nine-inch lengths of the leaking and neighboring tubes were removed. Sections of six tubes were sent to the Westinghouse R&D Center, Pittsburgh, Pennsylvania for metalurgical characterization. These consisted of the leaking tube (R42-C55) and five neighboring and previously plugged tubes (R44-C54, R43-C54, R44-C55, R43-C55 and R43-C56).

2.0 Nondestructive Examinations

Prior to removal of each section from the steam generator, a yellow dot was placed on each section to define the tube surface closest to the perimeter of the generator. In the current examination this dot was taken as the 0° position. Each tube length was received in one or two sections, originally extending from near the top of the tubesheet to ten in. above the top of the tubesheet.

Photographs of the leaking tube from Row 42 - Column 55 (R42-C55) show a "fish-mouth" opening at 0° and axially oriented flats at 0, 60 and 315°. These flats had circumferential striations, Figures 2-1 and 2-2. Photographs in Figures 2-3 to 2-8 are of the neighboring previously plugged tubes: R43-C55, R44-C55, R43-C54, R44-C54 and R43-C56. Similar flats were observed on all tubes at various angular positions. There is extensive metal loss and apparent deformation on all tube sections. Tubes from R44-C55 and R44-C54 arrived in two sections.

Wall thickness measurements were consistent with a nominal 50 mil wall away from the flats and a wall thickness reduction at the flats, Figure 2-9, Table 2-1.

Double wall x-ray radiographs were made of all tube sections at 0, 45, 90 and 315°. A Seifert Industrial X-ray unit was used with the following settings: 5 min. exposure time, 110 to 70 kV, 10 milliamperes, 60 in. source-to-film distance, large focal spot, and Kodak M-8 lead pack film. Wall thickness reductions were easily seen; however, there was no evidence of intergranular attack or stress corrosion cracking.

Prints of typical radiographs on the C55 tubes are shown in Figures 2-10 to 2-12, together with diagrams which depict the locations and orientations of the laboratory cuts that were made for microscopic examinations. The other three tubes were examined metallographically on transverse cross sections at elevations of 2-1/2 and 4 in. from the tops of the sections; cutting diagrams are not indicated for these three tubes. After cutting in the laboratory, all sections were notched at 0° on the tubesheet end to maintain orientation.

3.0 Metallography

The metallographic mounts are positioned on tubesheet maps in Figures 3-1 and 3-2 in an attempt to aid others in constructing the sequence of events leading to tube leakage.

Microstructures through the leaking tube R42-C55 are shown in Figures 3-3 and 3-4. These microstructures were etched with two percent bromine-methanol solution (only etchant used in this study). Cold work was not evident on the flat that burst, but was apparent on the 60° flat. The fracture face was not intergranular and was of the tensile overload type. The microstructure appeared normal and had carbide banding occurring to a greater degree near the I.D. At O.D. surfaces away from the flats, shallow amounts of cold work were observed and probably resulted from belt polishing in the manufacture of the tubing, e.g., 0.2 mils depth of cold work at 270° in Figure 3-4.

Metallography on the other tubes is presented in Figures 3-5 to 3-17 and the depth of cold work on the flats is summarized in Table 3-1. Thirty eight of forty examinations of the flats showed evidence of cold work up to a depth of 1.1 mils. One of the two flats not showing evidence of cold work was at 0° on tube R42-C55 and was the flat that ruptured. The heaviest degrees of cold work were observed on the bottom of the concave surface of R44-C55, Figures 3-9 to 3-11. Some transgranular cracks were present and may have resulted from fatigue. Microhardness traverses, Figure 3-18 and Table 3-2, confirmed that the 0° flat on tube R42-C55 had no detectable cold work and that O.D. surfaces away from flats and other flats had cold work (increase in hardness at the surface).

4.0 Scanning Electron Microscopy

Examinations were made of surfaces with the scanning electron microscope (SEM - also used to designate scanning electron micrograph) and with the Energy Dispersive X-ray Spectrometer (EDS). For tube R42-C55, the flat that ruptured had circumferential striations, and the fracture surface had some dimples that are characteristic of tensile overload, Figures 4-1 and 4-2.

Fractography on a horizontal fracture near the center of R43-C55 suggested that fatigue contributed to cracking, Figures 4-3 and 4-4.

On tube R44-C55, an EDS analysis on a flat was rich in Al, Si, Cr, Fe, Cu and Zn as compared to Inconel 600, Figure 4-5. The fracture surfaces near the bottom of the tube were not well defined and contained deposits, Figures 4-6 to 4-9.

Other fractographs on R44-C54 indicated that fatigue contributed to the fracture, Figures 4-10 and 4-11.

5.0 Composition and Mechanical Properties of Tubes

An EDS analysis of Section 1A of tube R44-C55 indicated that the principal elements were within specification. The mechanical properties of the Inconel 600 tubing were estimated and tabulated in Table 5-1. Knoop (500 g) hardness readings were made mid-wall on the metallographic mounts 4 inches down on Tubes R42-C55 and R44-C55. These were converted to Rockwell "B", R_B , readings which were then used to estimate yield strength by two methods. One was a correlation established previously on Inconel 600 tubing, Figure 5-2, and the other was an International Nickel Company correlation on Inconel 600 sheet and strip. Reasonable agreement existed between the two conversions: all estimates of yield strength were between 45,000 and 62,000 psi. An estimate of ductility of the Inconel tubing was obtained with bends. Rings 7A, 7B and 7C from Tube R44-C55 and 7A and 7B from tube R42-C55 were used. Each ring was positioned such that a location free of flats between 1450 and 2250 would be at the apex of a U-bend. The bend was made by placing the ring over a 3/32 in. diameter mandrel with a line of contact at the designated position and deforming the ring at this location around the bar. This strained the O.D. circumference in tension. No fissures were observed on the O.D. surface at the apex and the calculated outer fiber strain was twenty-eight percent.

6.0 Conclusions

1. The microstructure and mechanical properties of the burst tube and a neighboring plugged tube were determined and were normal for the mill annealed Inconel 600 tubing material.
2. There was no evidence of stress-corrosion cracking or intergranular attack on I.D. or O.D. surfaces of any tube.
3. All tubes displayed flat zones of O.D. wall reduction with circumferential striations within the flats.
4. Thirty-eight of the forty flats that were studied showed cold work on the O.D. surface, indicating that a wear process produced the flats.
5. The "fish-mouth" burst occurred at a flat where the wall thickness had been worn to 0.008 in. from the nominal 0.050 in. original wall; cold work was not identified on this flat.

6. The fracture of the "fish-mouth" was consistent with a tensile overload failure.
7. The most severe cold work was observed on a concave indented surface at the bottom of a peripheral tube R44-C55.
8. Fatigue striations were identified on fractures associated with breakage of two of the previously plugged tubes.

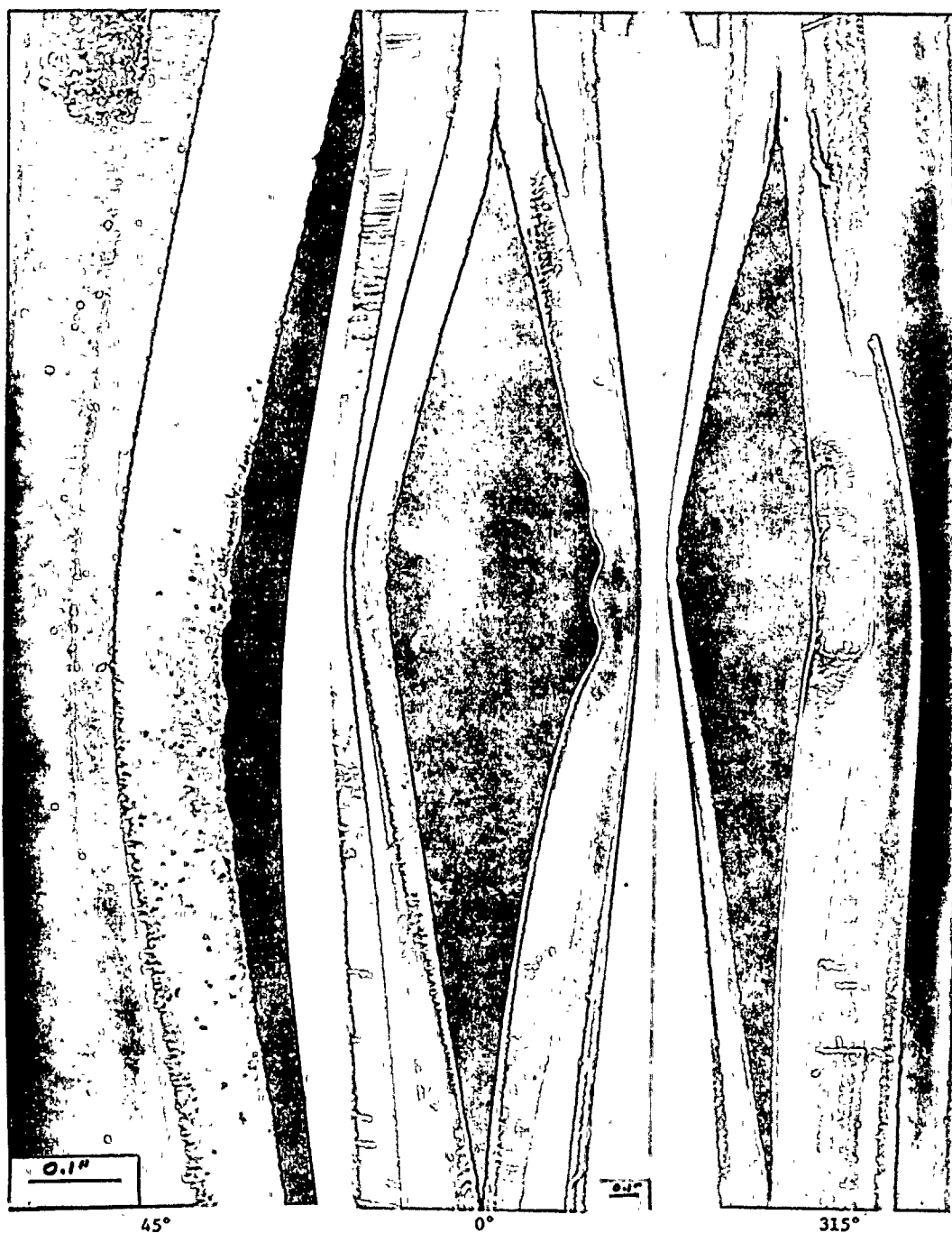


Fig. 2-1. Fish mouth crack at near 0° on Tube R42-C55 from RGE (GINNA), SGB, hot leg

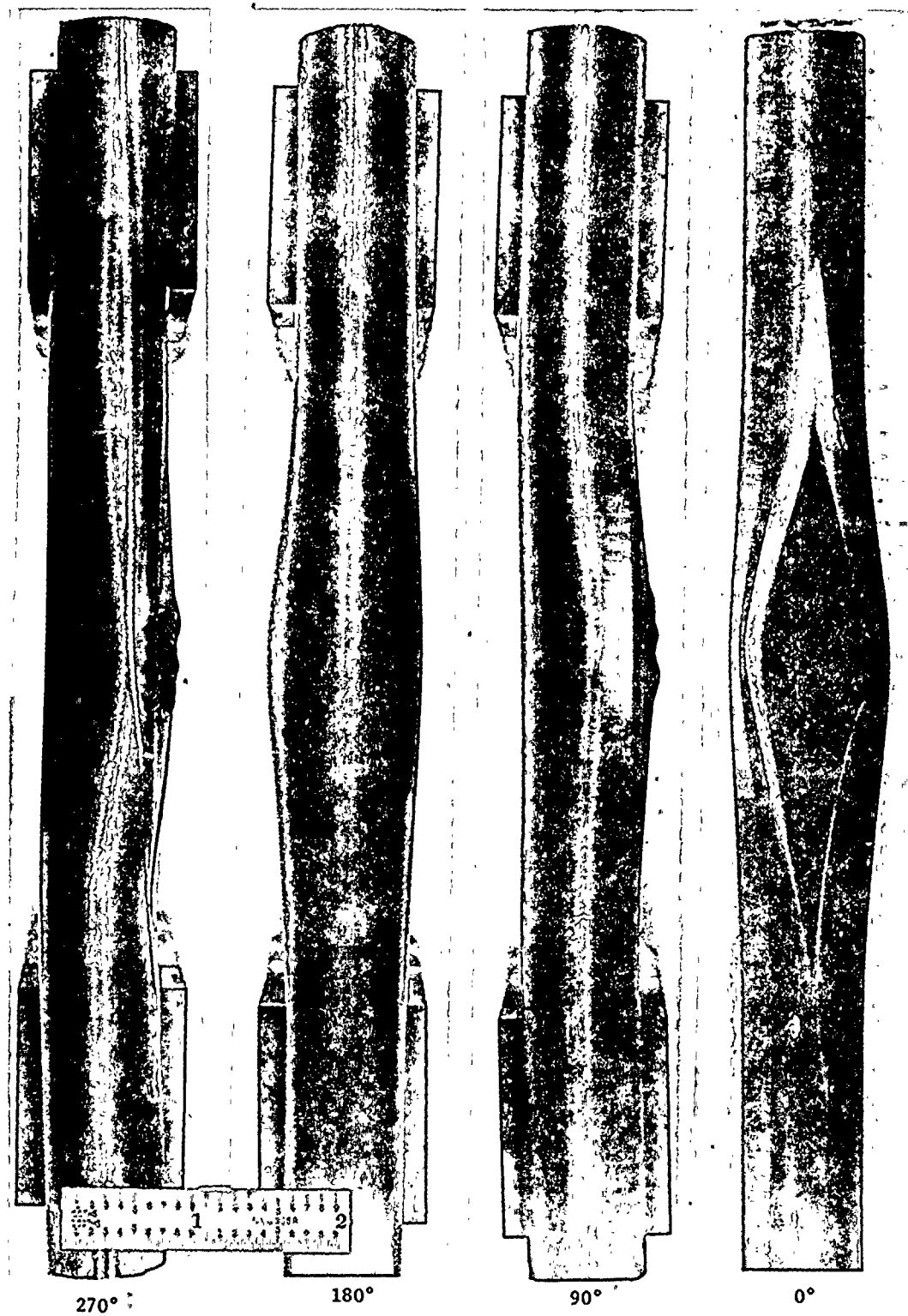


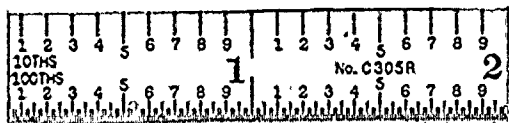
Fig. 2-2. Tube R42-C55 from RGE (GINNA), SGB, hot leg



Fig. 2-3. Tube R43-C55 from RGE (GINNA), SGB, hot leg



Fig. 2-4. Tube R44-C55 from RGE (GINNA), SGB, hot leg



315°



180°



90°



0°

Fig. 2-5. Tube R44-C55 from RGE (GINNA), SGB, hot leg



Fig. 2-6. Tube R43-C54 from RGE (GINNA), SGB, hot leg



Fig. 2-7. Tube R44-C54 from RGE (GINNA), SGB, hot leg



Fig. 2-8. Tube R43-C56 from RGE (GINNA), SGB, hot leg

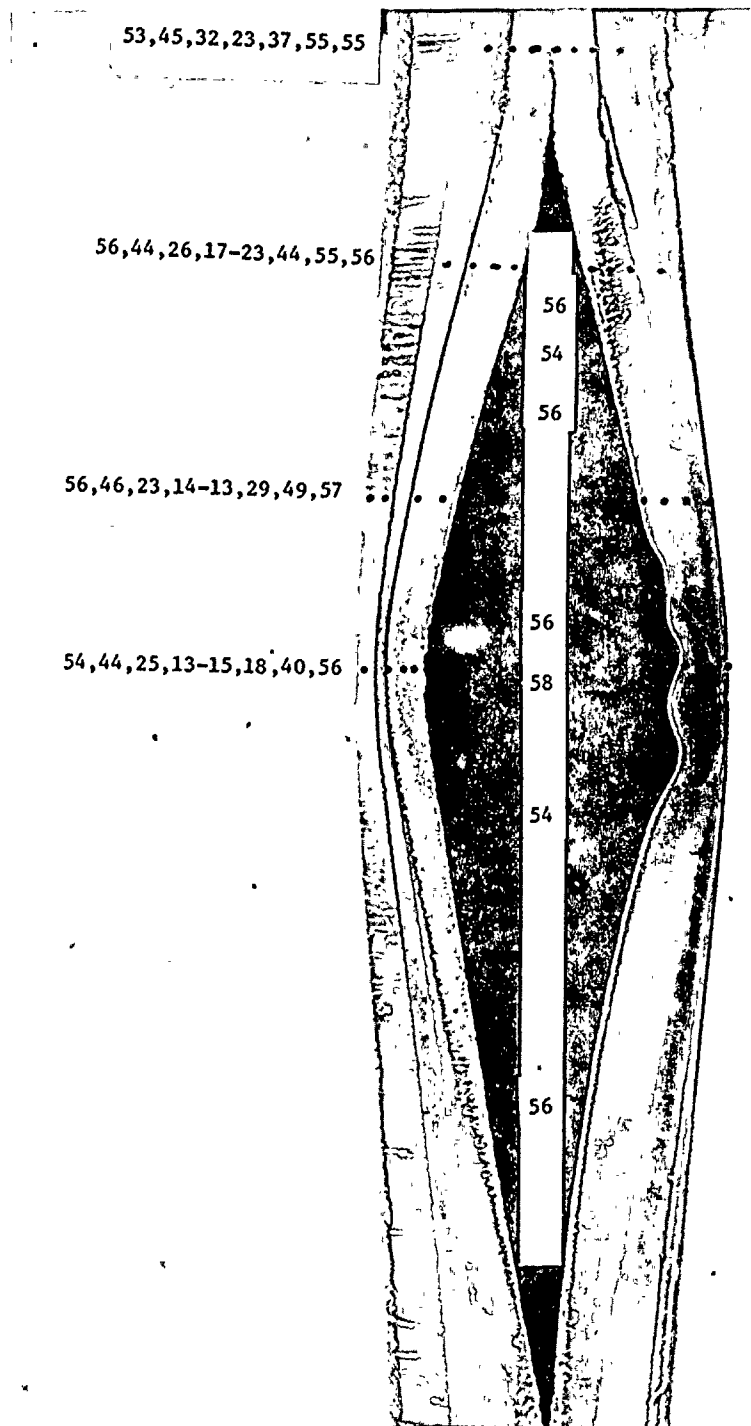


Fig. 2-9. Wall thickness measurements (mils) superimposed on 0° photograph of R42-C55

Table 2-1

Wall thickness measurements (mils) at various positions
on Column 55 tubes

Tube No. (Axial position)	Angular Position							
	0°	45	90	135	180	225	270	315
R42								
(1/2" below top)	50	54	53	54	56	57	51	57
(1/2" above bottom)	56	53	53	53	53	54	56	56
(1/4" above bottom)	57	53	53	53	52	--	--	--
R43								
(1/2" below top)	47	46	51	52	53	51	48	10
(1/2" above bottom)	---	46	53	47	49	--	56	--
R44								
(1/2" below top)	53	53	51	50	50	45	30	53
(3/4" above bottom)	48	--	--	--	--	--	--	--
(1/2" above bottom)	46	--	--	--	--	--	--	--
(1/4" above bottom)	36	--	--	--	--	--	--	--

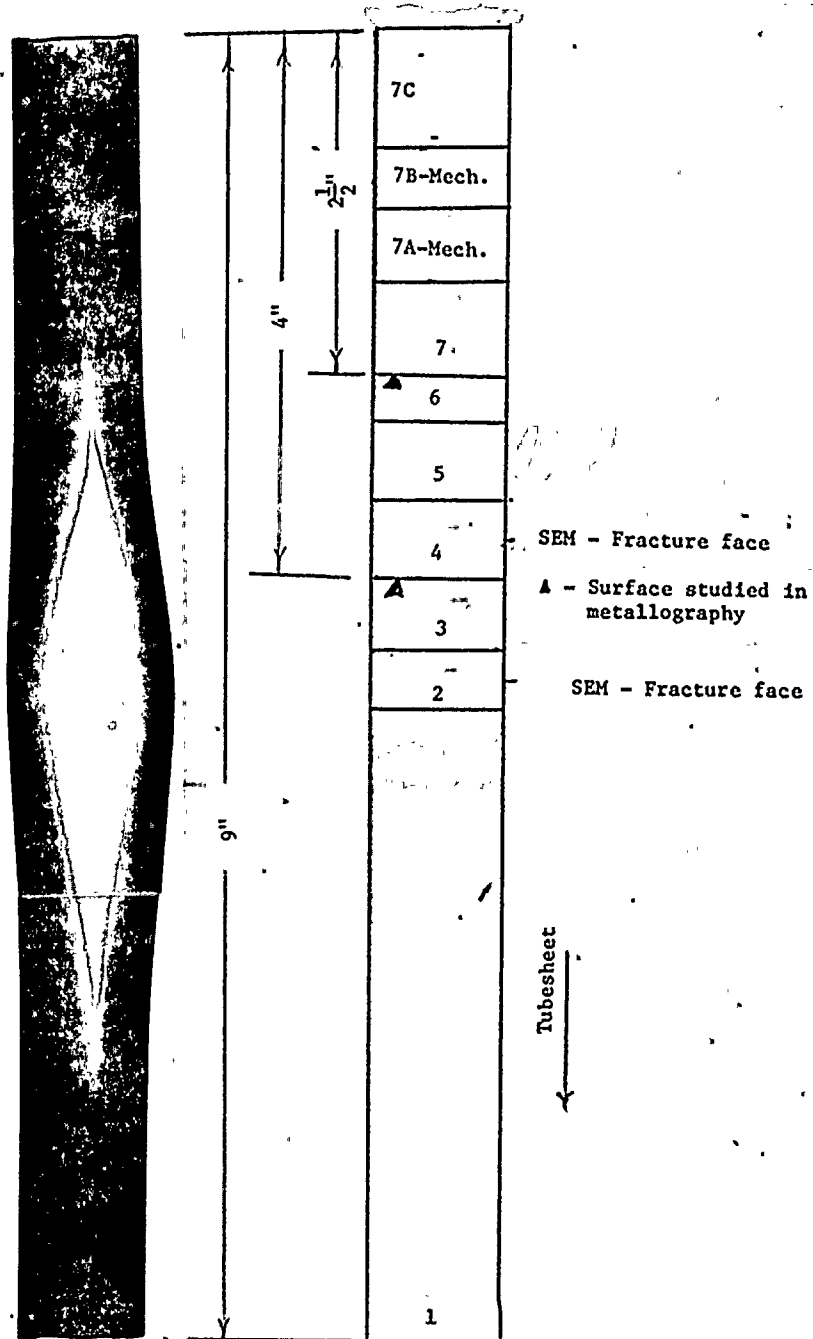


Fig. 2-10. Print of double wall X-ray radiograph at 0° for Tube R42-C55 and diagram showing cuts, section identification, and sample use.

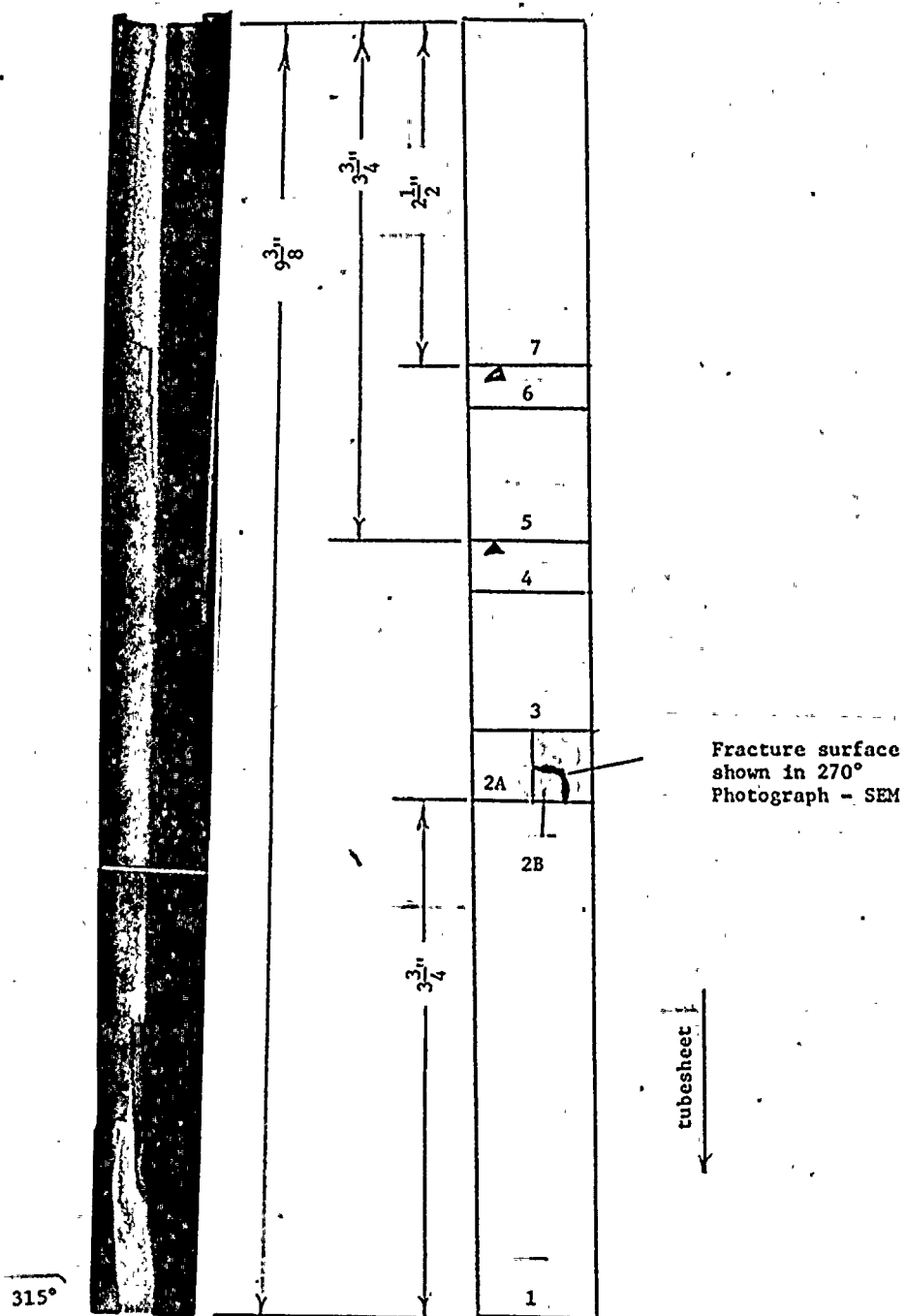


Fig. 2-11. Print of double wall X-ray radiograph for Tube R43-C55 and cutting diagram

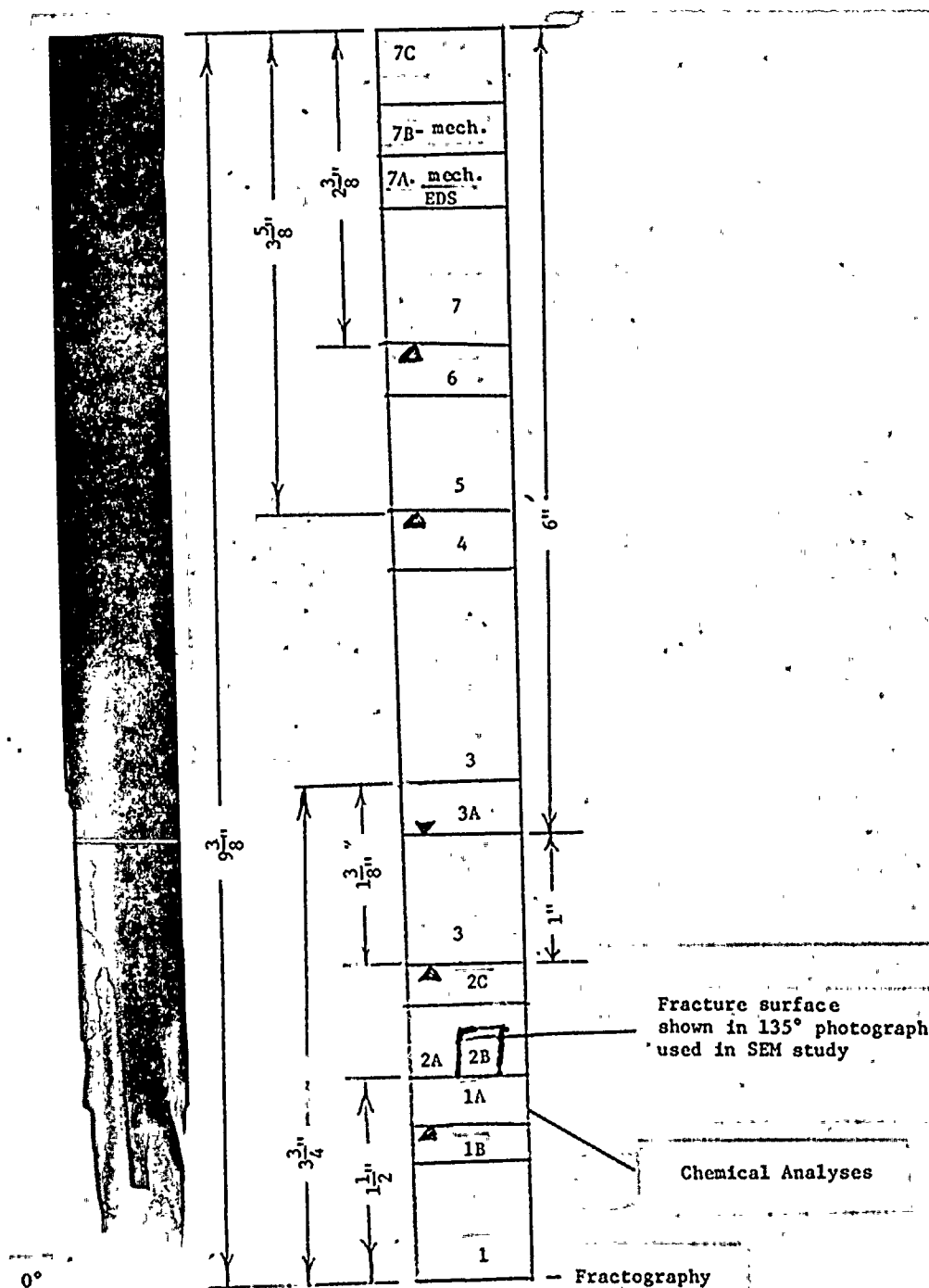


Fig. 2-12. Print of double wall X-ray radiograph at 0° for top portion of Tube R44-C55 and cutting diagram

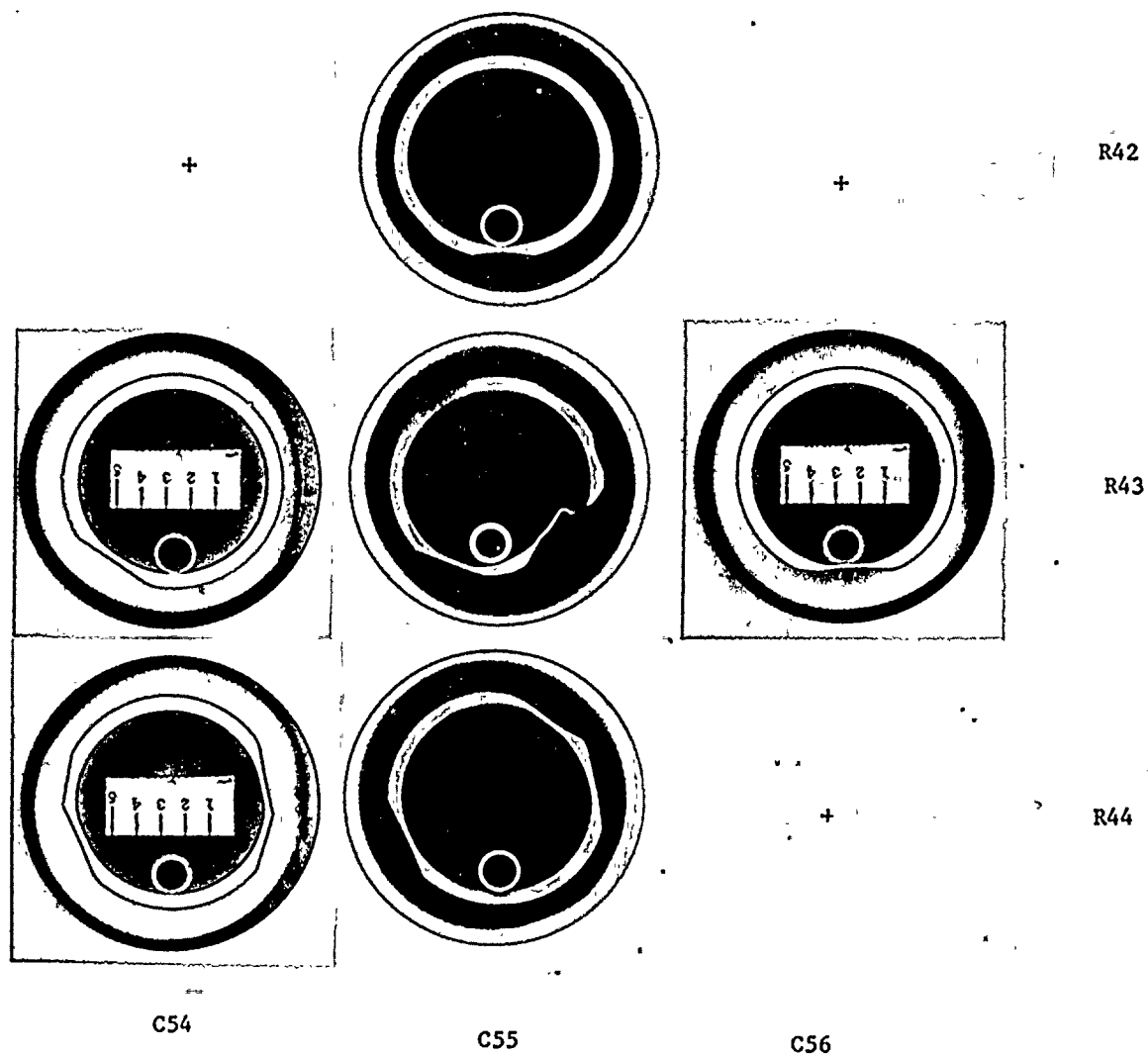


Fig. 3-1. Transverse cross-sections at $\sim 2\frac{1}{2}$ " from tops of the sections (Small circle designates 0°)

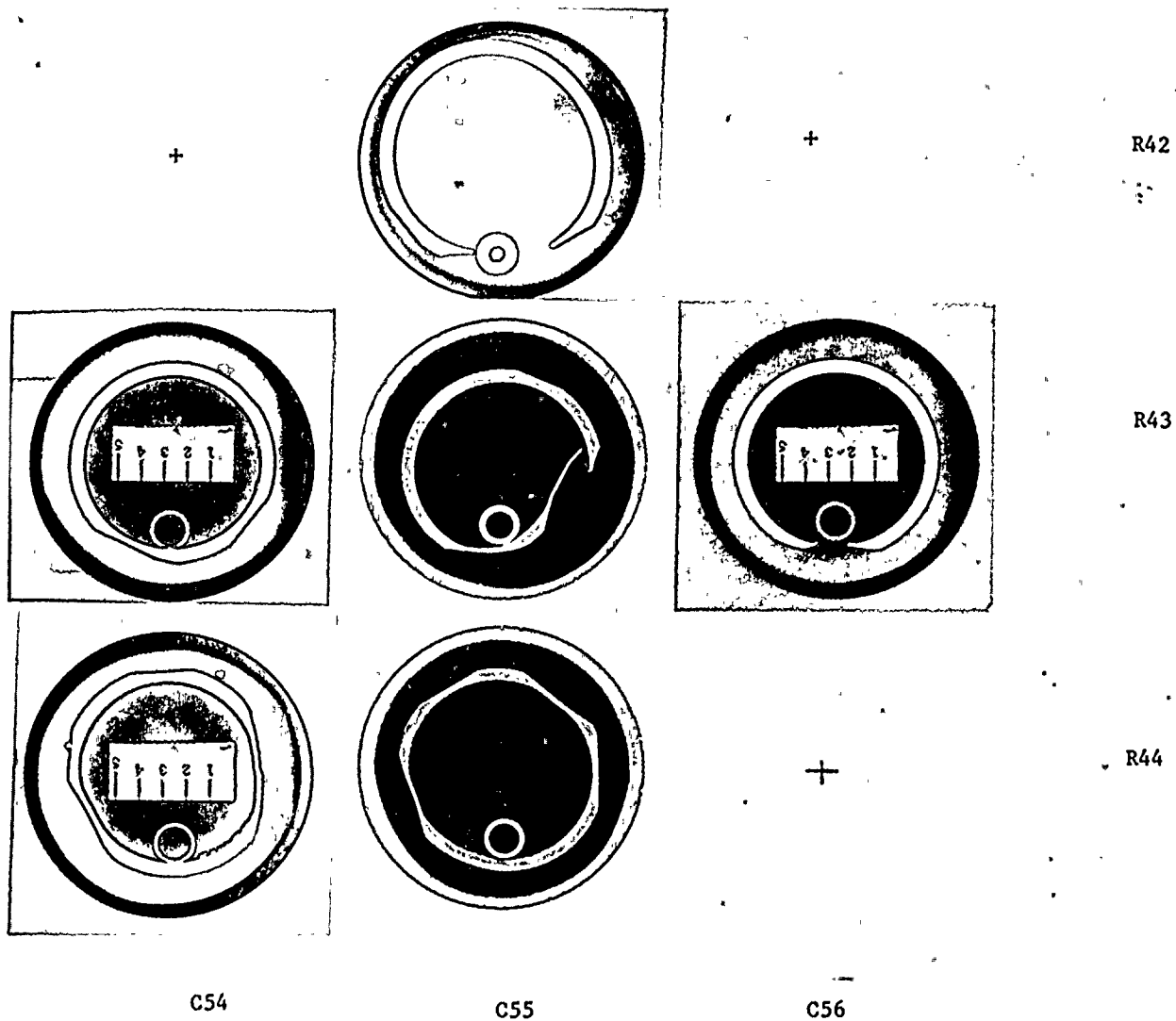


Fig. 3-2. Transverse cross-sections at $\sim 4''$ from the tops of the sections

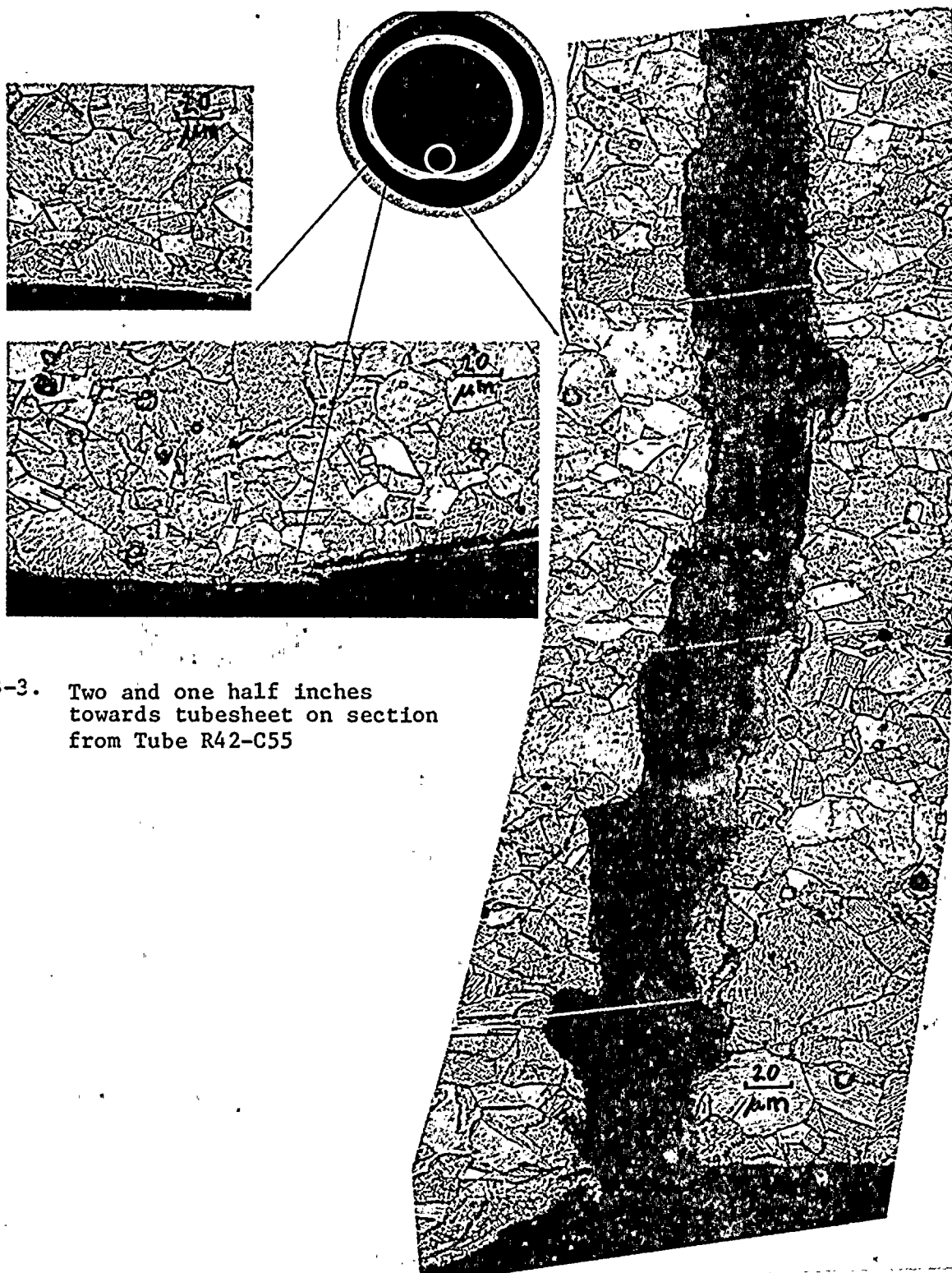


Fig. 3-3. Two and one half inches
towards tubesheet on section
from Tube R42-C55

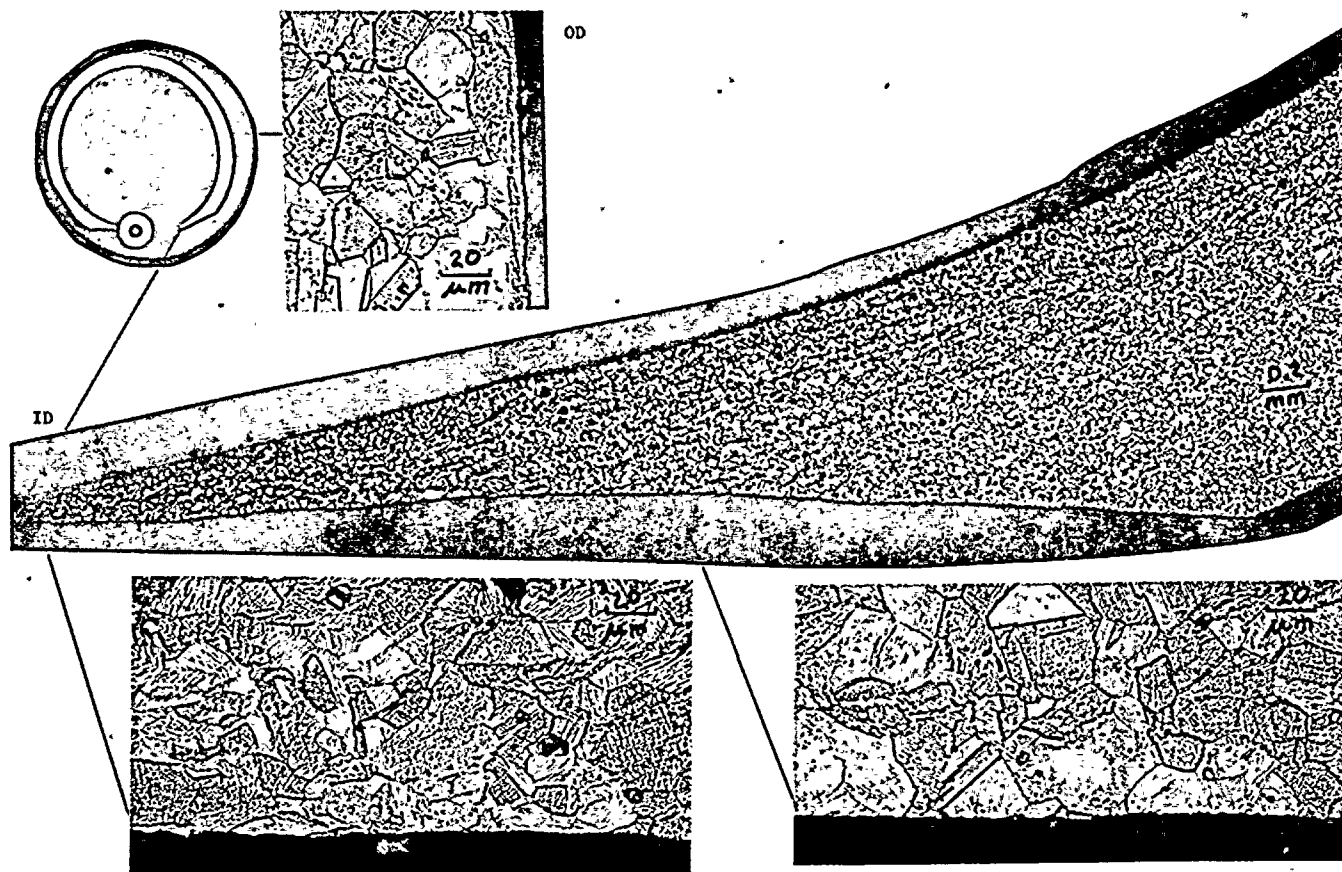


Fig. 3-4. Metallography on transverse cross-section ~4" towards tubesheet
on section from Tube R42-C55

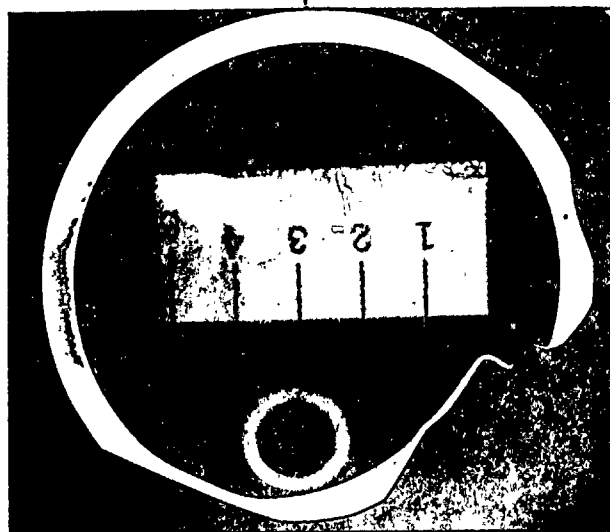


Fig. 3-5. OD surfaces $2\frac{1}{2}$ " down from the top of the section from Tube R43-C55

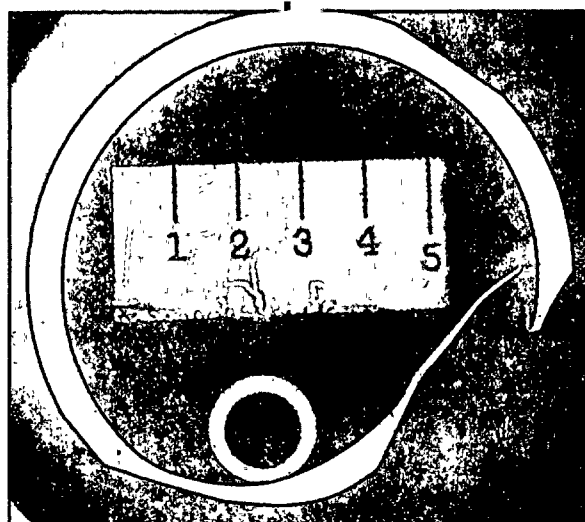


Fig. 3-6. OD surfaces 4" down from the top of the section from Tube R43-C55

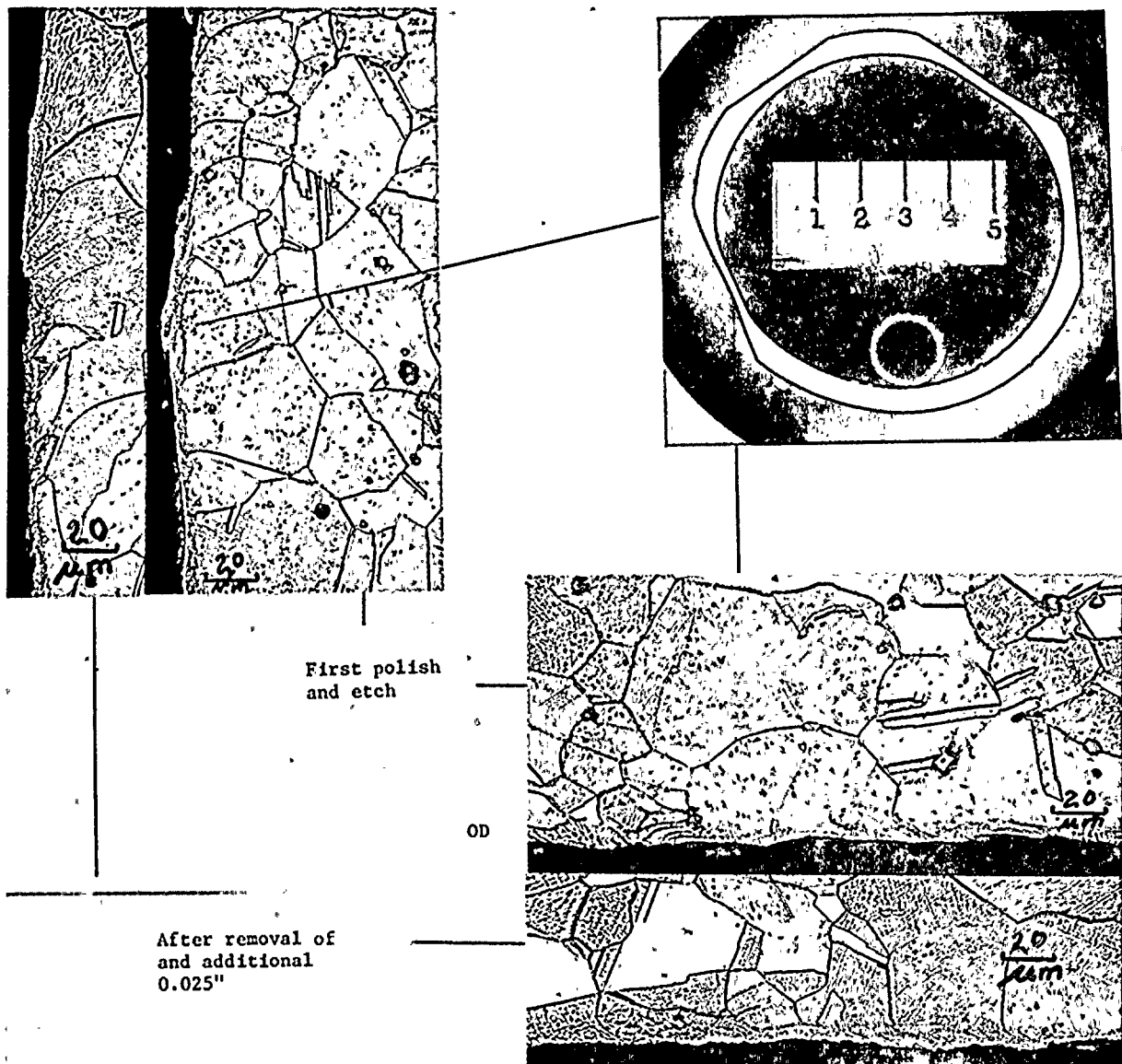


Fig. 3-7. Four inches down from top portion of Tube R44-C55

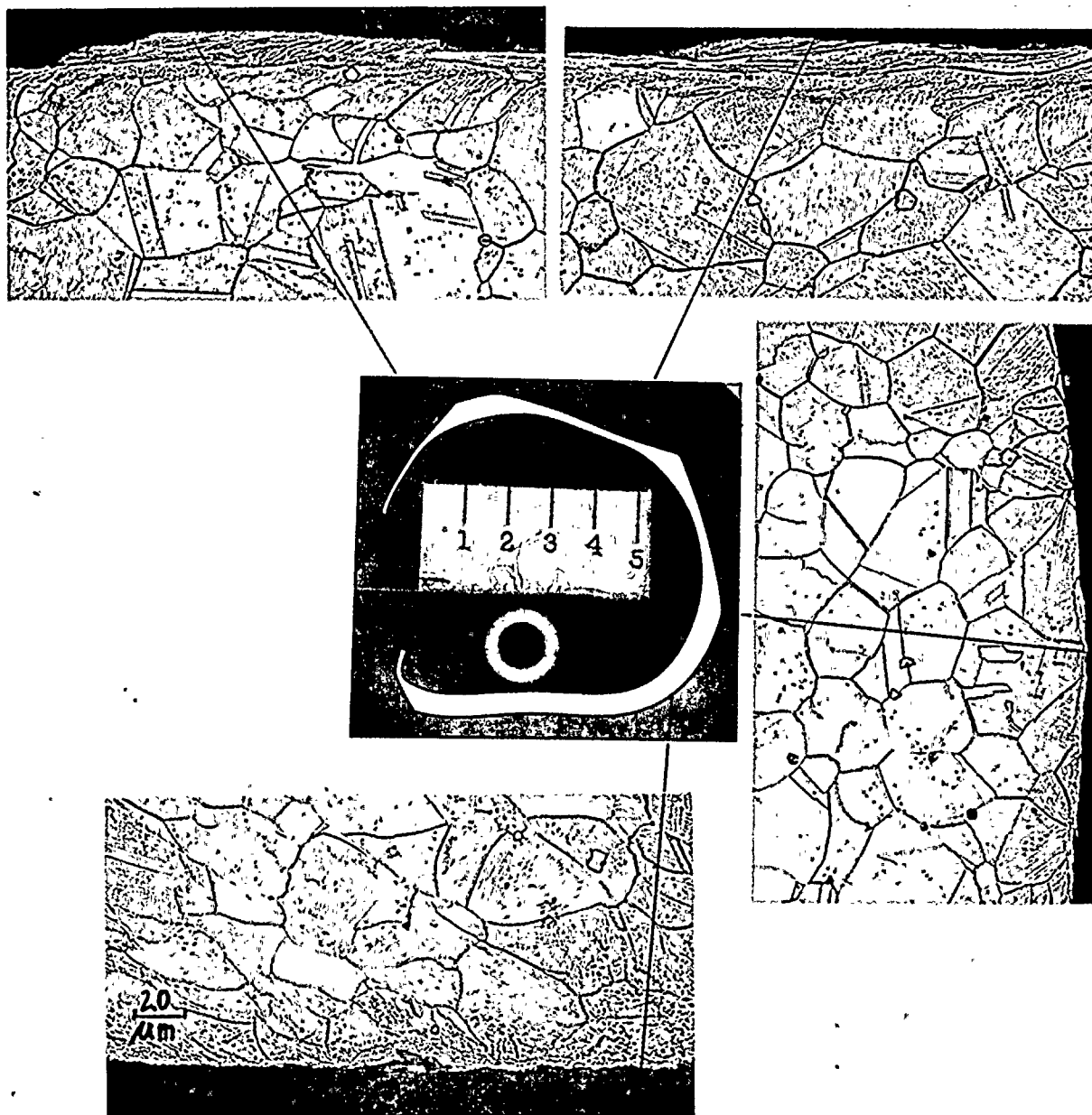


Fig. 3-8. Metallography on transverse cross-section down 6" from top of top portion of Tube R44-C55. Similar results were observed after polishing an additional 24 mils.

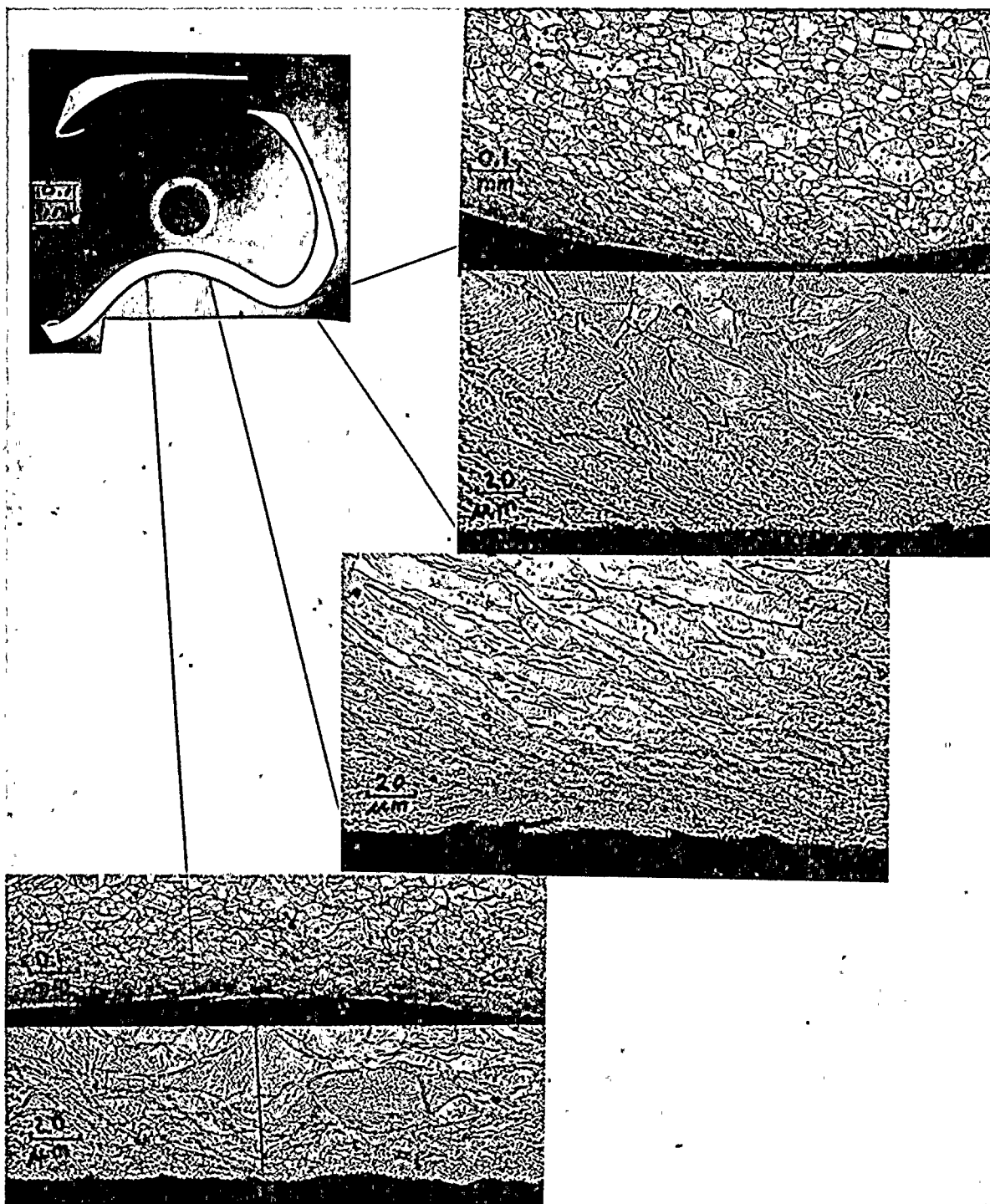


Fig. 3-9. Metallography 7" from top of top portion of Tube R44-C55

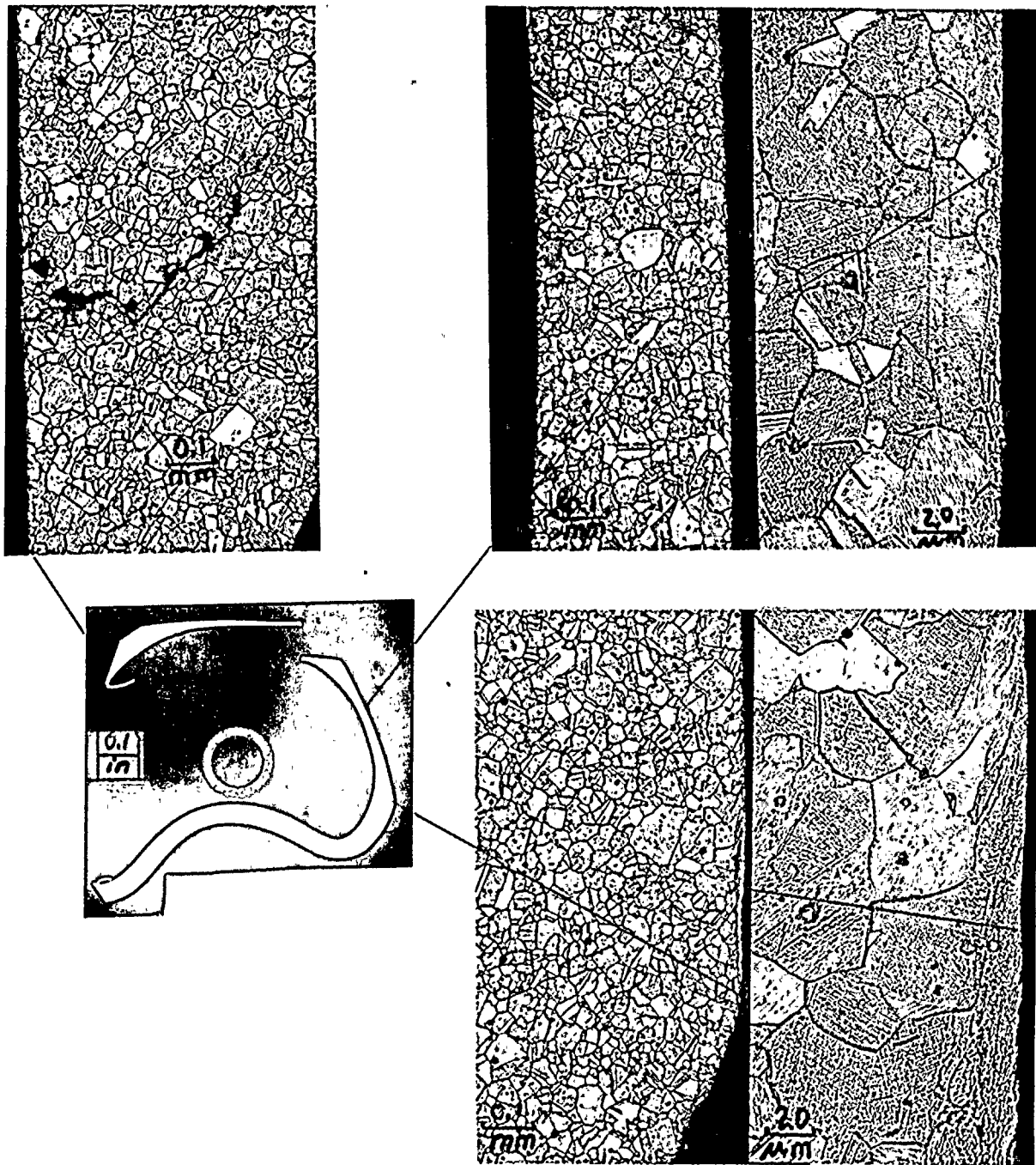


Fig. 3-10. Continuation of metallography 7" from top of top portion of Tube 344-C55

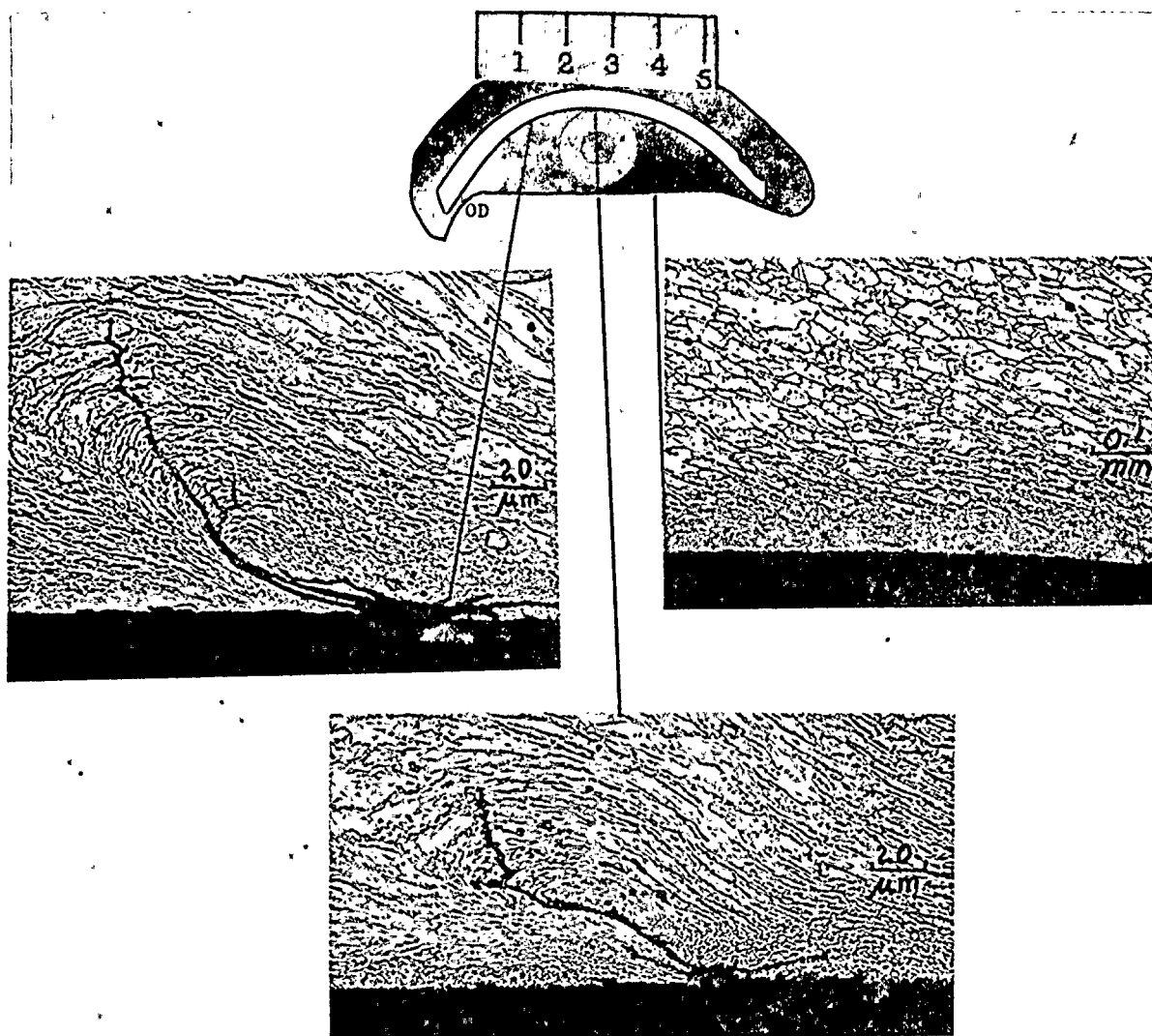


Fig. 3-11 . Metallography at the OD (0°) $8\frac{1}{4}$ " down from the top of the top portion of R44-C55

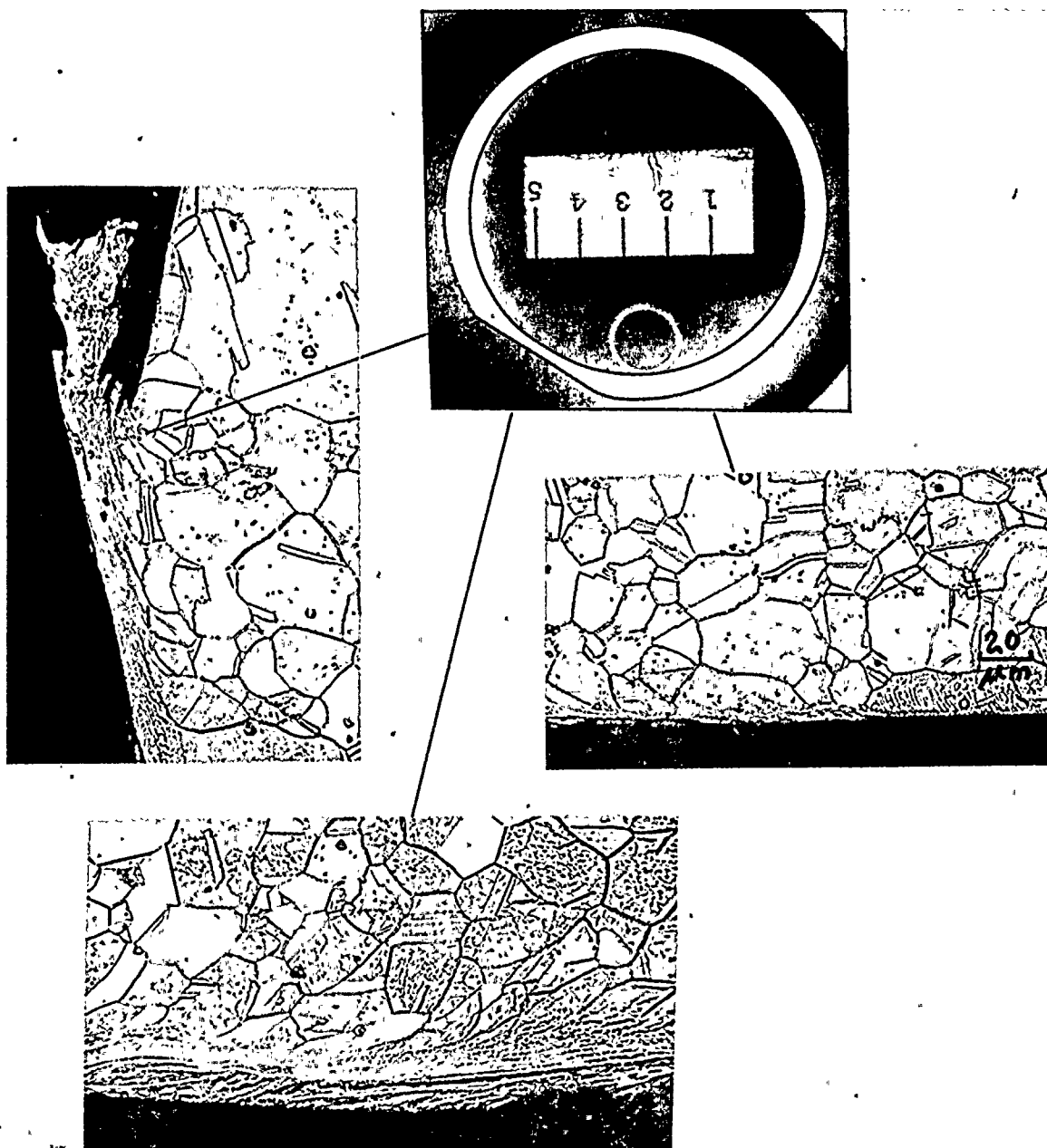


Fig. 3-12. Metallography $2\frac{1}{2}$ " down from the top of section from Tube R43-C54

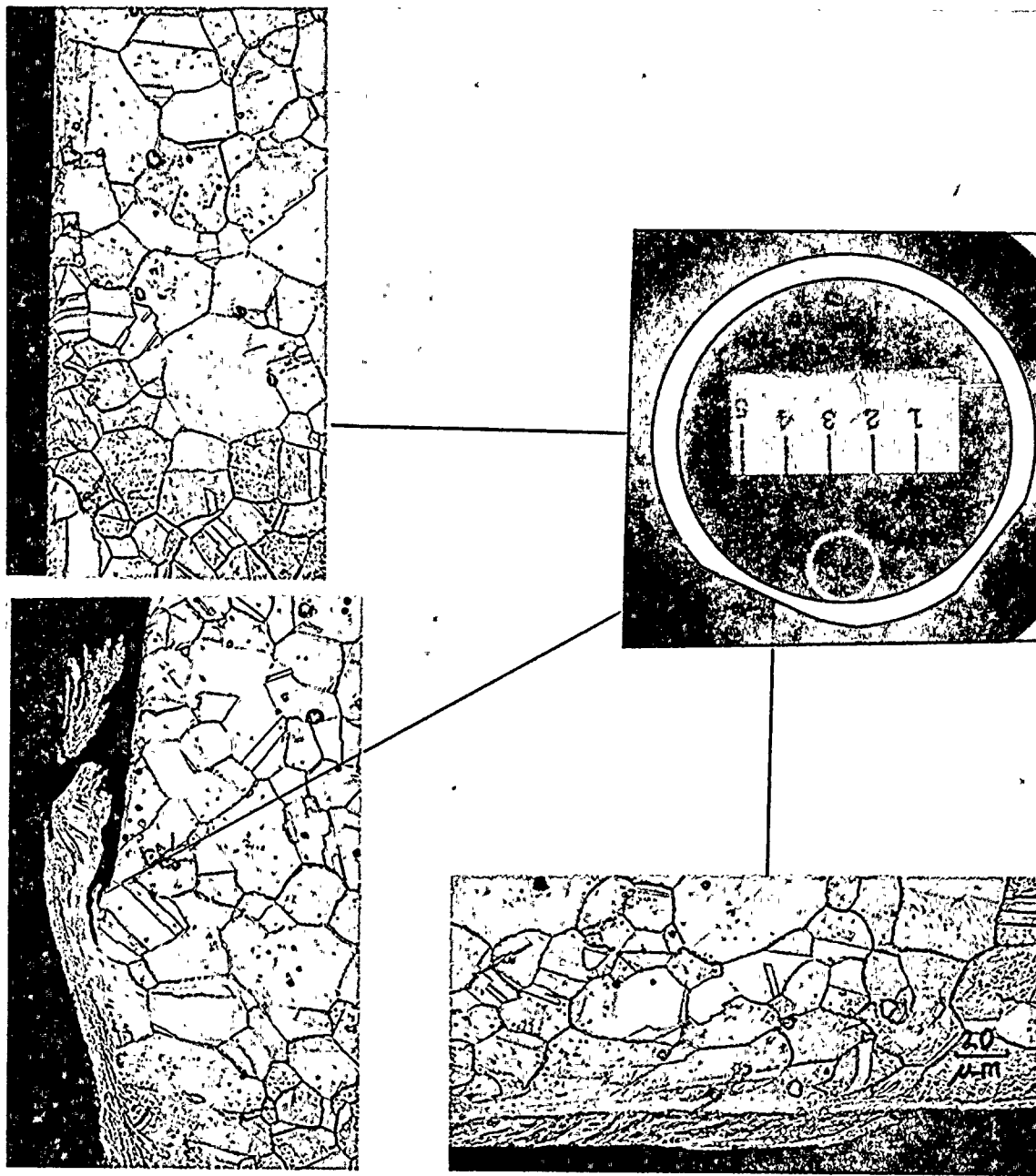


Fig. 3-13. OD surfaces $3\frac{3}{4}$ " down from top of section from
Tube R43-C54

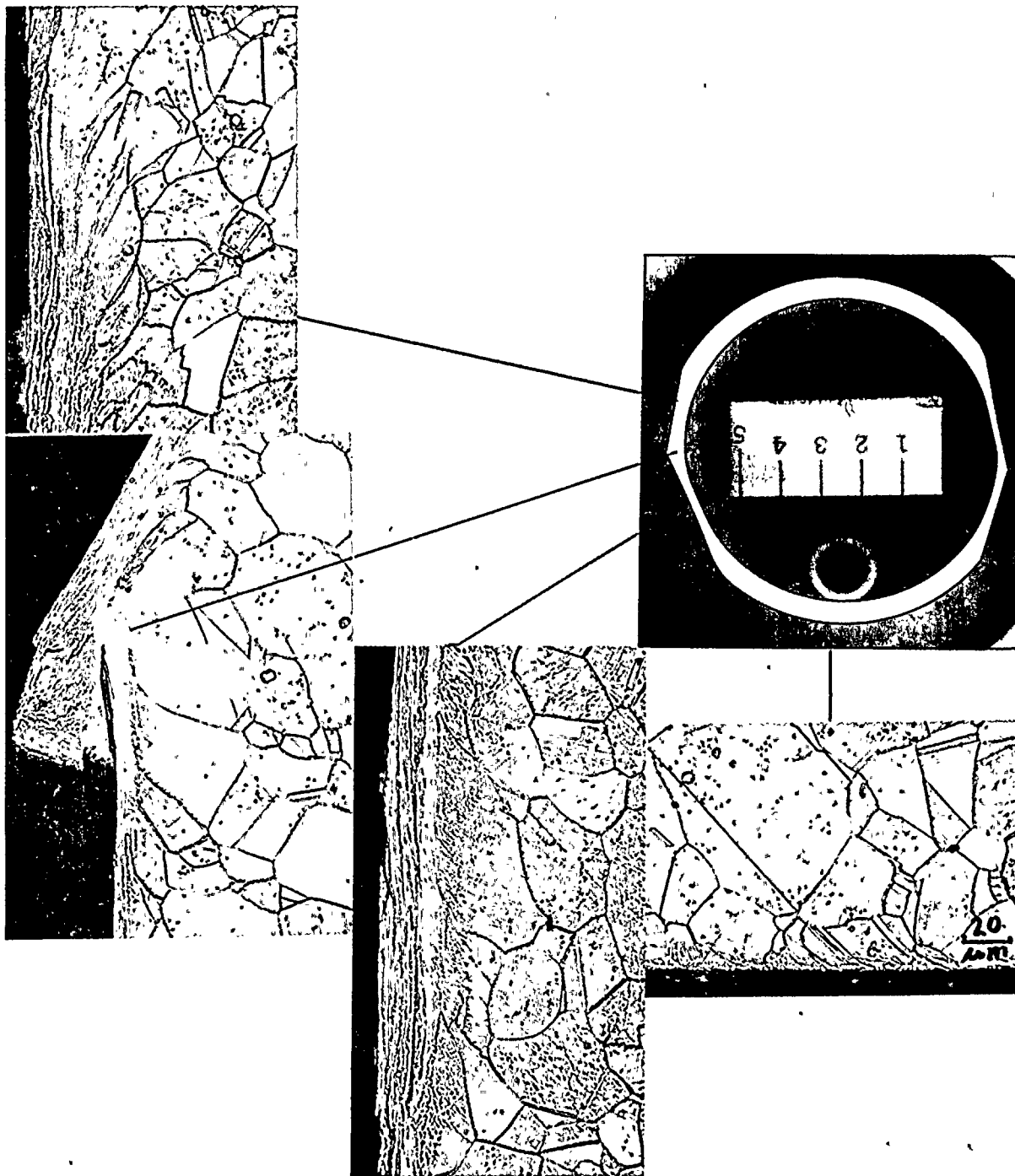


Fig. 3-14. Transverse cross-section $2\frac{1}{2}$ " down from the top of the top portion of Tube R44-C54

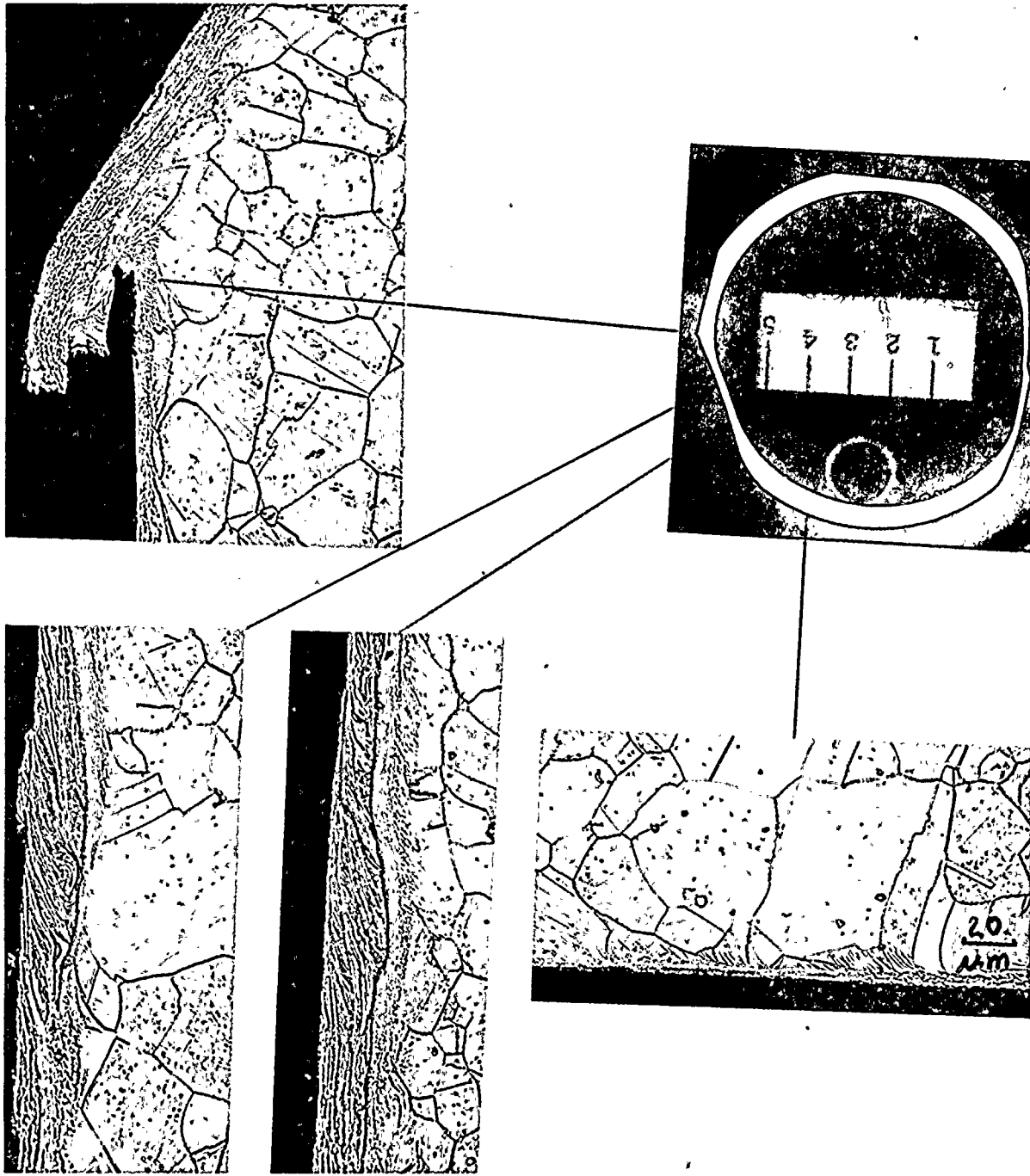


Fig. 3-15. Metallography $3\frac{3}{4}$ " down from top end of top portion of R44-C54

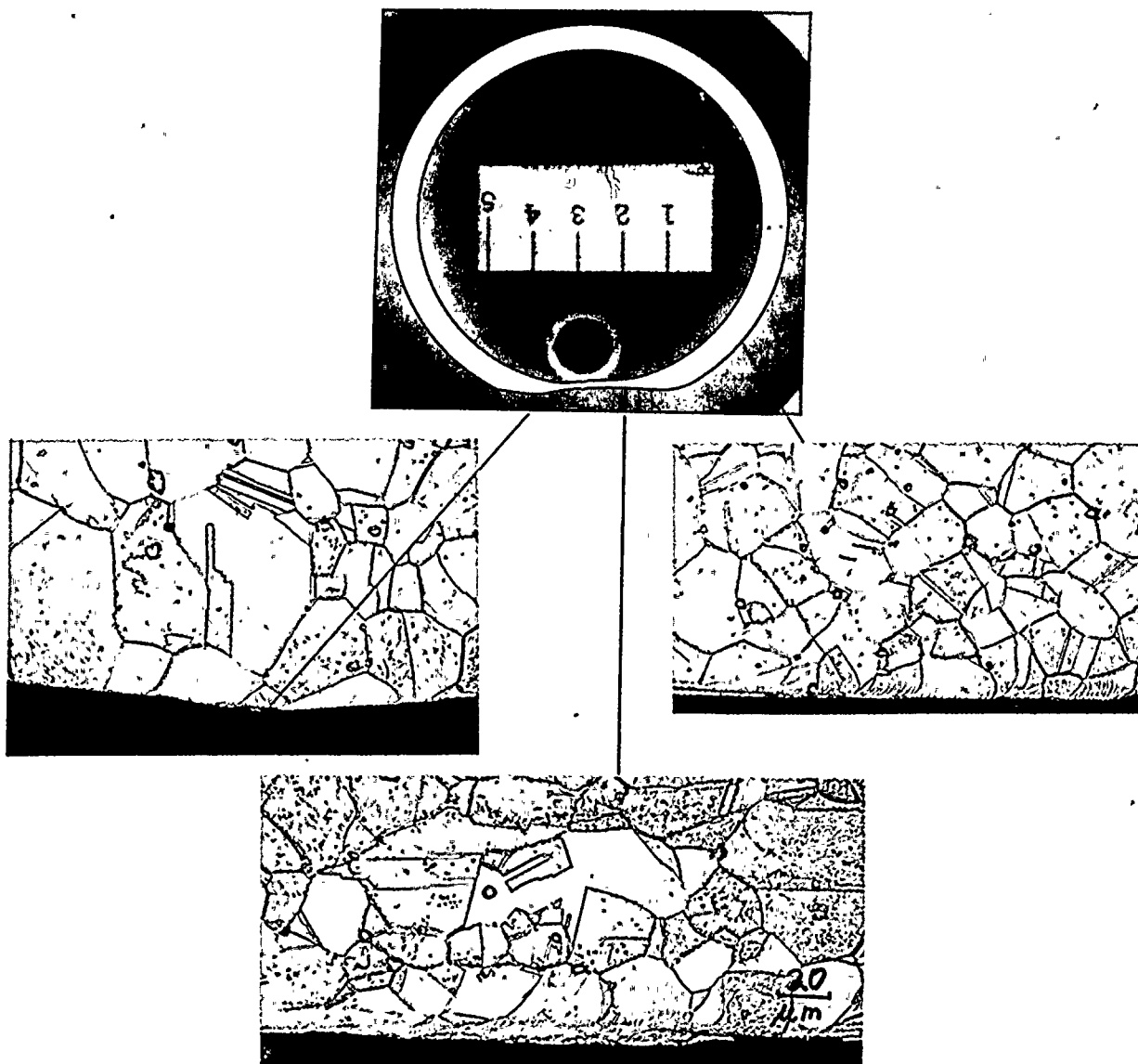


Fig. 3-16. OD surfaces $2\frac{1}{2}$ " down from the top of the section from Tube R43-C56

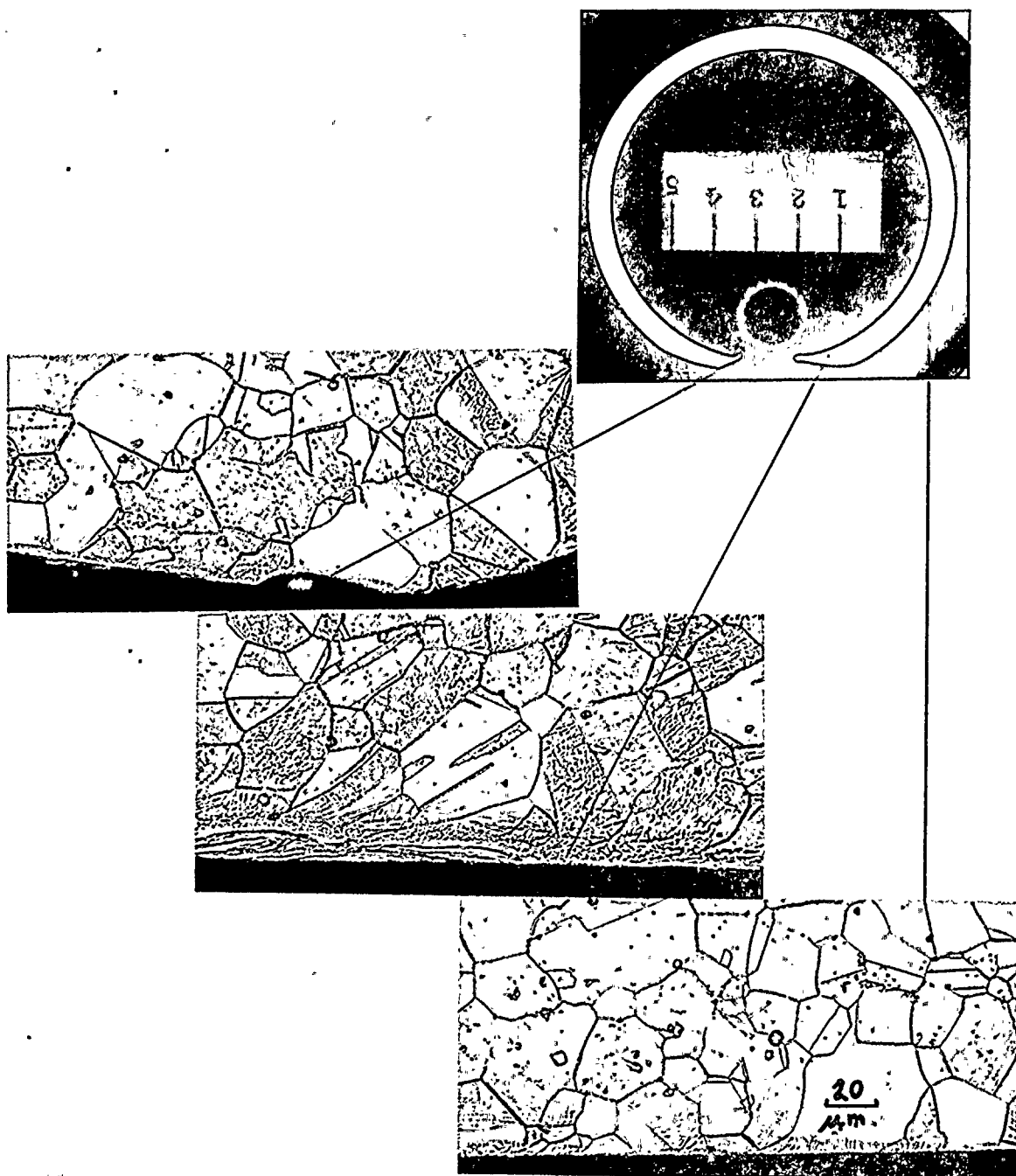


Fig. 3-17. OD surfaces $3\frac{3}{4}$ " down from the top of the section from
Tube R43-C56

Table 3-1

Depth of cold work to the nearest 0.1 mil on wall reduced areas (Tabulated values are angular position-max. depth in mils)

Tube No.
(Approximate
Axial Position
From Top of
Tube Section)

R42-C55

2-1/2" (0° - 0.0)* (60° - 0.4)*
4" (0° - 0.0)* (60° - 0.4)

R43-C55

2-1/2" (30°-1.3) (225°-0.5) (270°-0.4) (330°-0.2)
4" (30°-0.3) (45°-0.5) (225°-0.5) (300°-0.4)

R44-C55

2-1/2" (60°-0.5) (225°-0.6) (270°-0.3)
4" (75°-0.2)* (105°-0.2) *(150°-1.0) (200°-0.6) (270°-0.4)
6" (105°-0.5) (150°-0.8)* (270°-0.6)*
7" (90°-0.0)*(180°-0.5) (240°-0.6)*

R43-C54

2-1/2" (30-0.9)*
4" (30°0.9)*(195°-0.5) (315°-0.5)

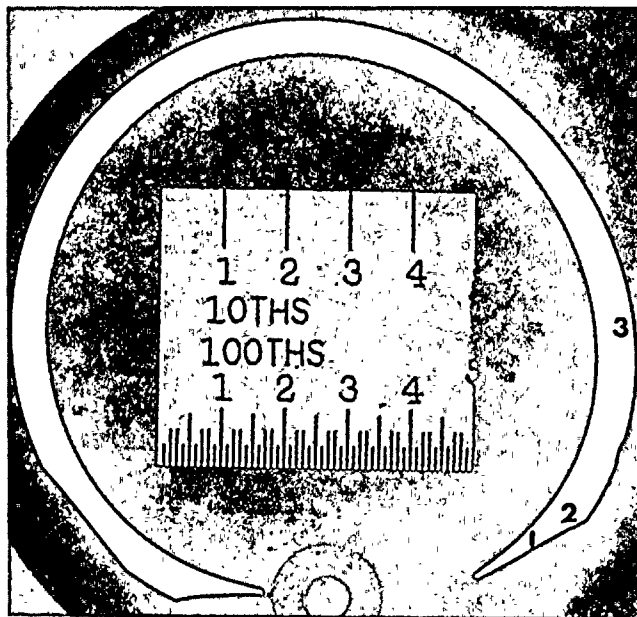
R44-C54

2-1/2" (60°-0.9)*(90-1.0)*(270°-0.6) (300°-0.9)
4" (60°-1.1)*(105°-1.0)*(180°-0.6) (270°-0.7)

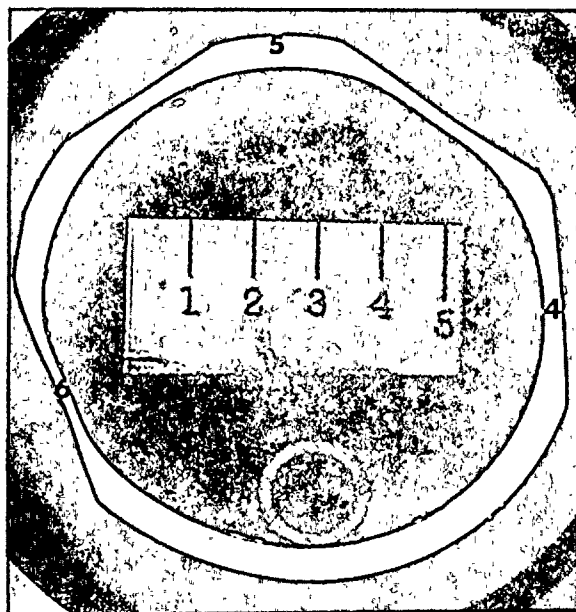
R43-C56

2-1/2" (0°-0.3)*
4" (0°-0.5)*

*Shown in photomicrographs on transverse cross-sections



Four inches from top of R42-C55



Four inches from top of R44-C55

Fig. 3-18 Locations of Knoop microhardness traverses

Table 3-2
Knoop (100g) microhardness traverses at
various locations on Tubes R42-C55 and R44-C55

Tube	Position No.	Remarks	~ Depth from OD surface in mils					
			1	2	4	9	14	19
R42-C55	1	Flat	224	228	231	237	--	--
	2	Flat	180	194	195	192	--	--
	3	No Flat	258	224	229	219	--	--
R44-C55	4	Flat	321	300	223	224	254	--
	5	No Flat	364	261	312	289	261	209
	6	Flat	321	312	248	214	226	194



Fig. 4-1 SEM's of flat and fracture face above center of fish mouth crack on Tube R42-C55

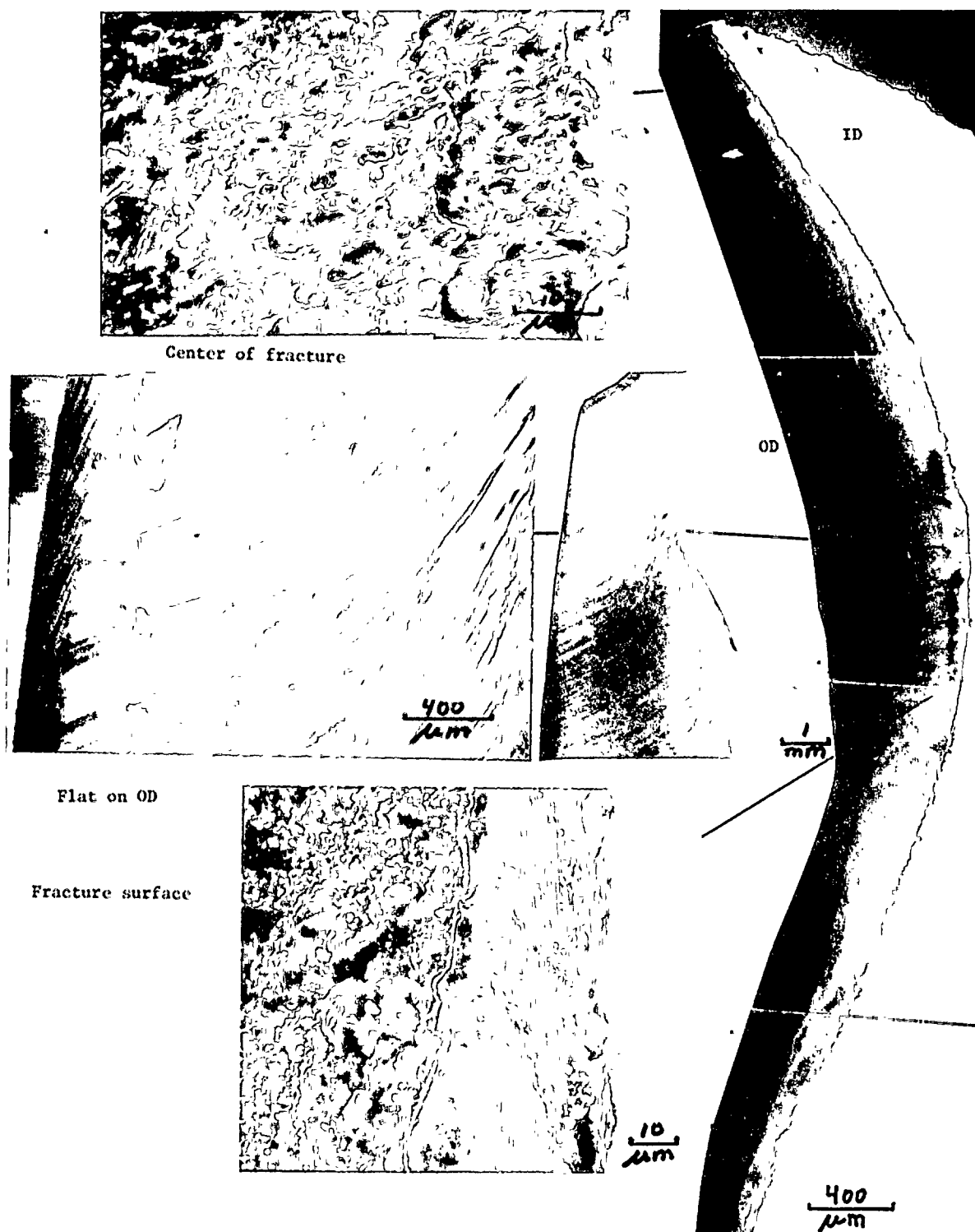
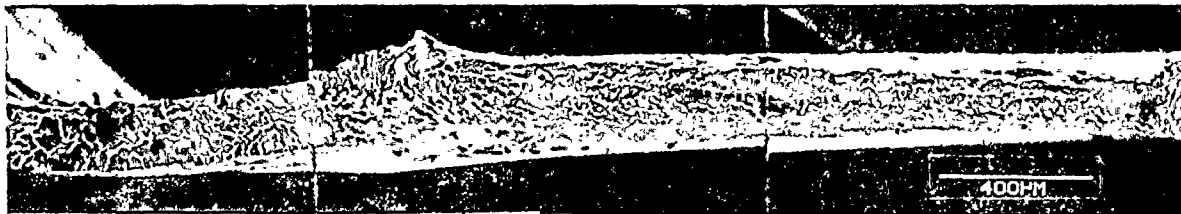


Fig. 4-2 SEM's of flat and fracture surface at center of fish mouth crack on Tube R42-C55



Higher magnification SEM's on next figure

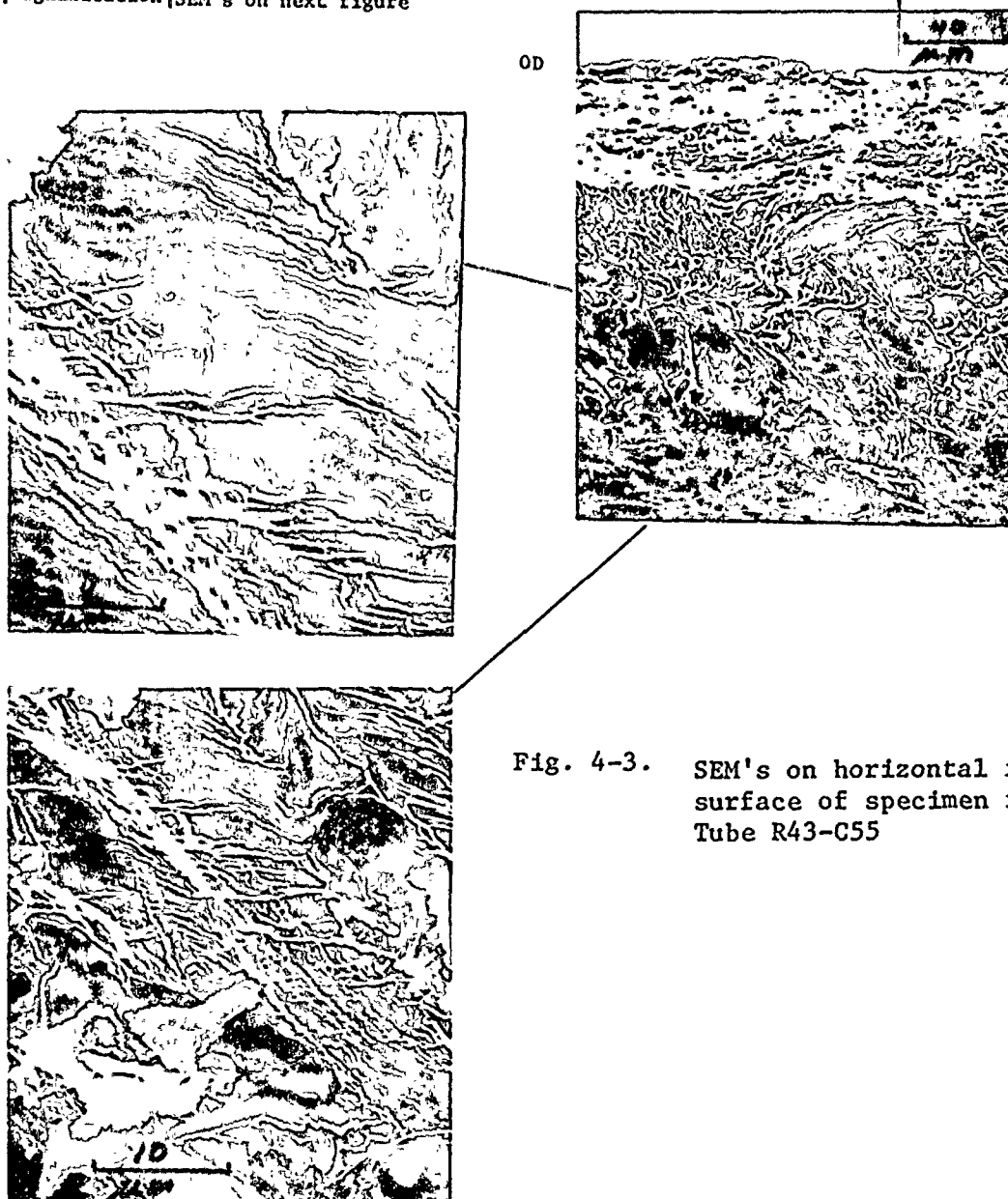


Fig. 4-3. SEM's on horizontal fracture surface of specimen from Tube R43-C55

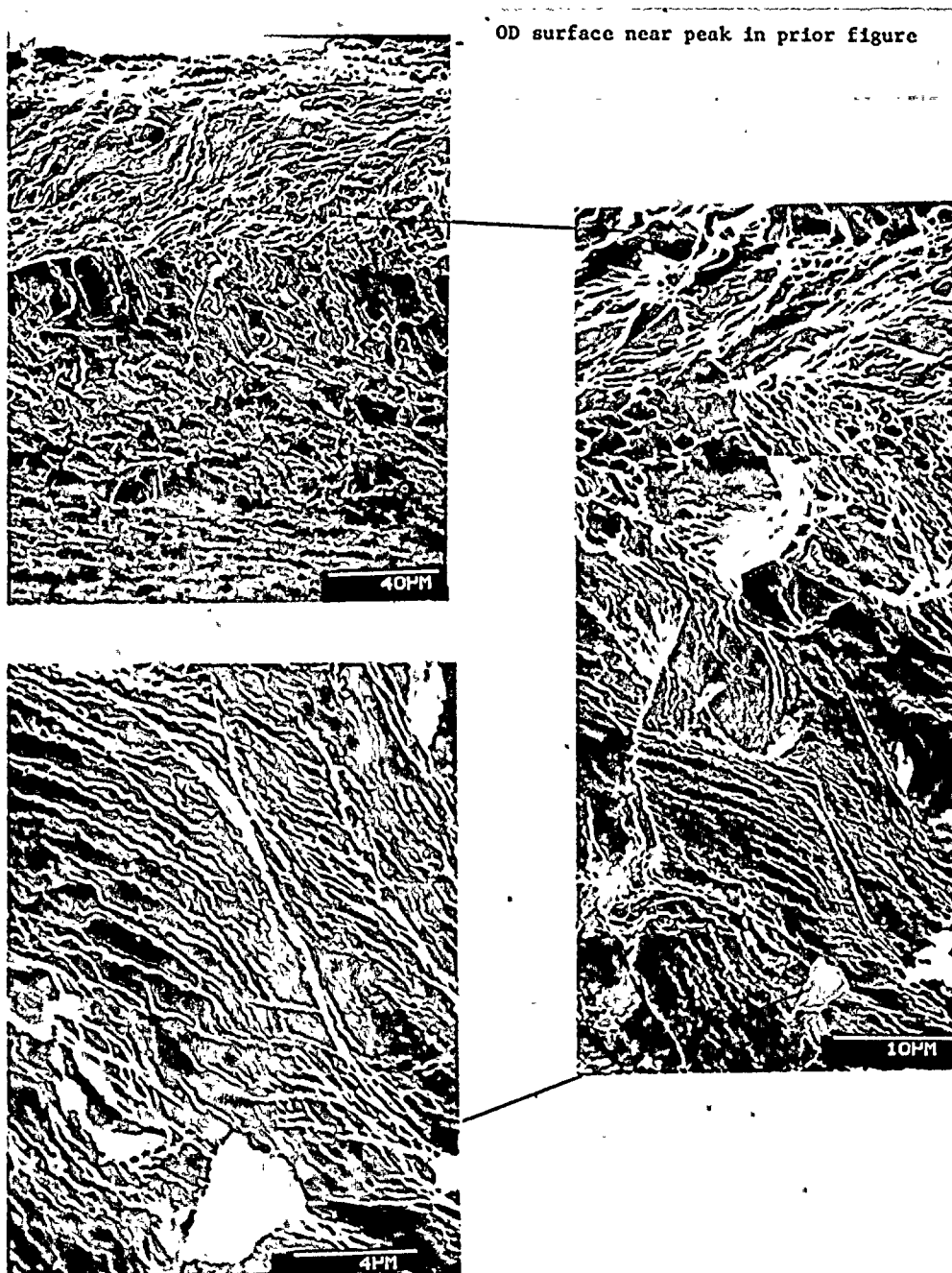


Fig. 4-4. SEM's near peak in prior figure and on fracture face.

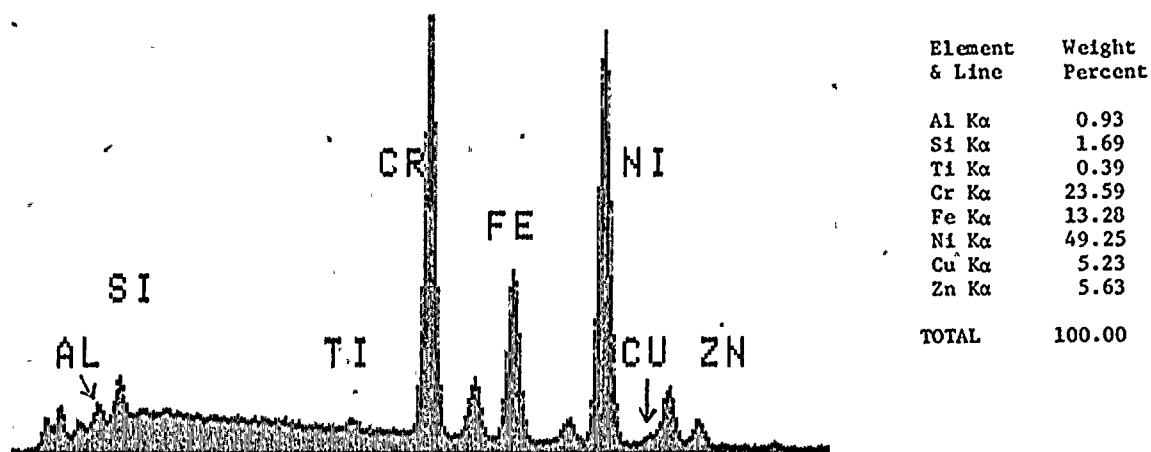
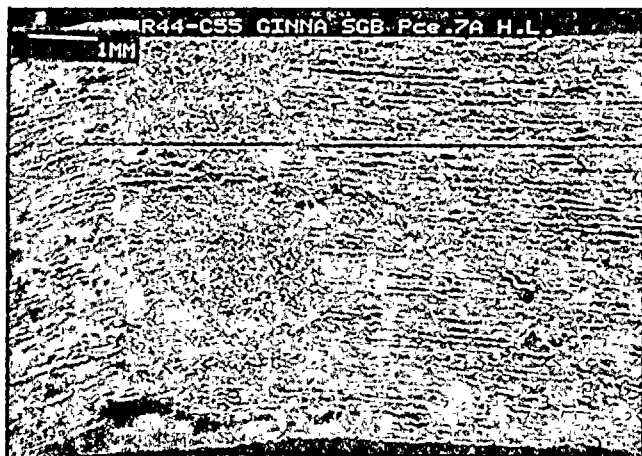


Fig. 4-5. EDS analysis on lower left area of 270° flat that was 1" down from the top of top portion of Tube R44-C55 (Section 7A).

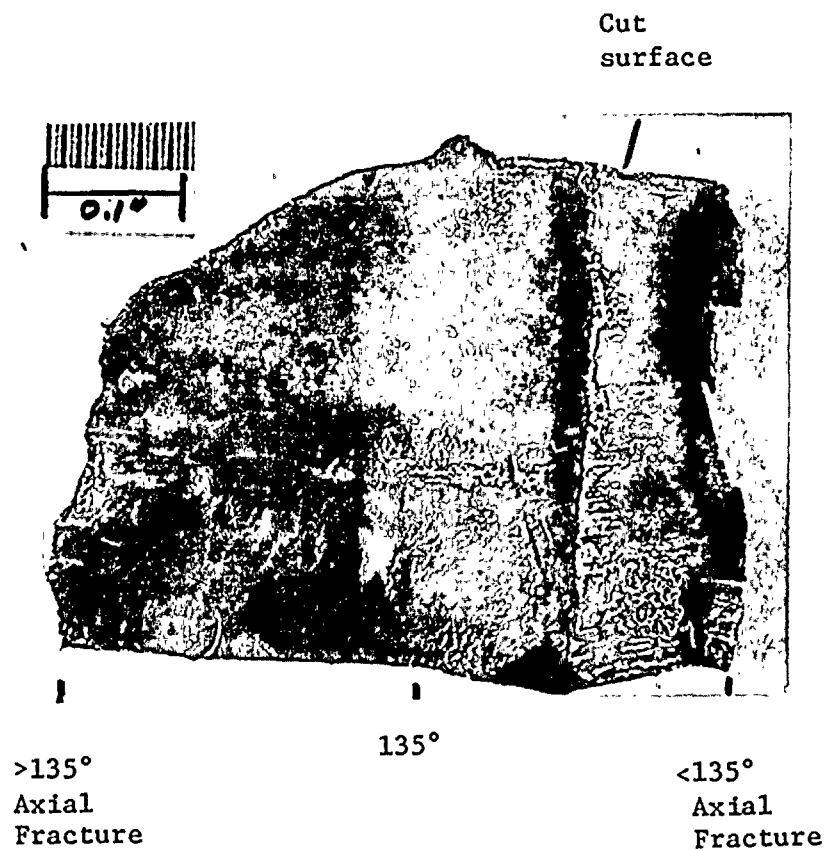


Fig. 4-6. Fractography was performed on two axial fracture surfaces 1-1/2" from the bottom of the top portion of Tube R44-C55

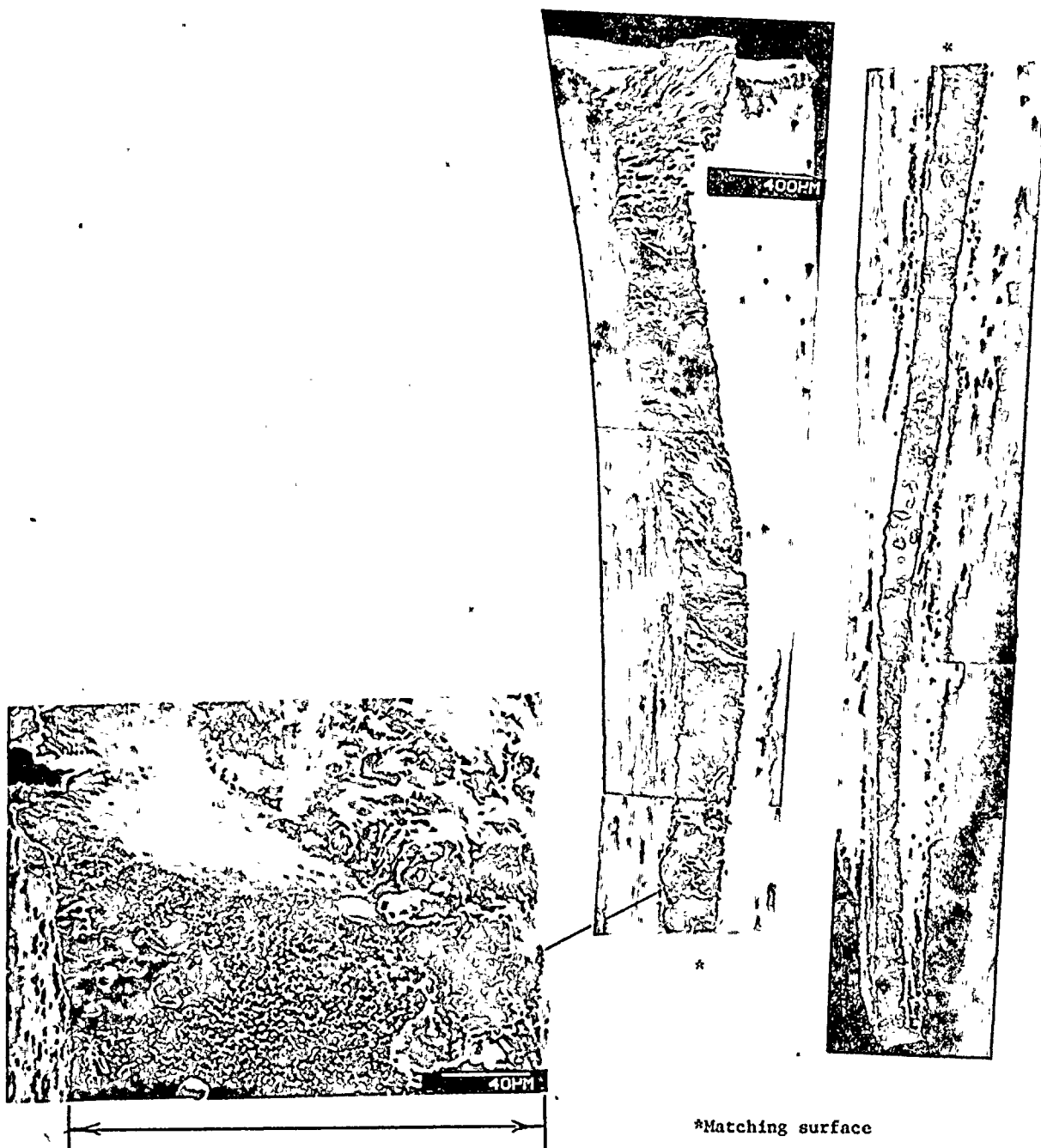


Fig. 4-7. Fractography on $>135^\circ$ axial fracture

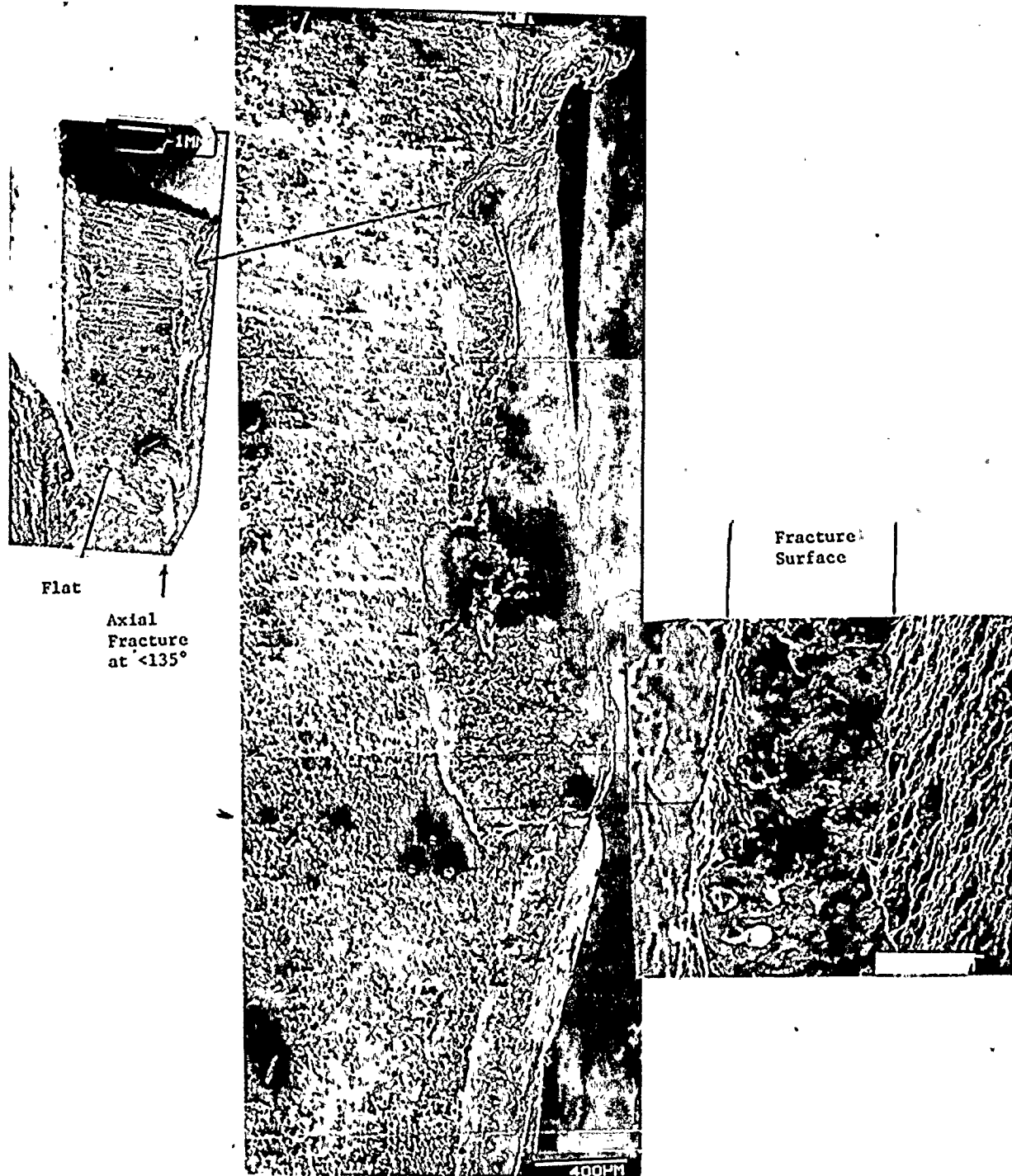


Fig. 4-8 Fractography on $<135^\circ$ axial fracture

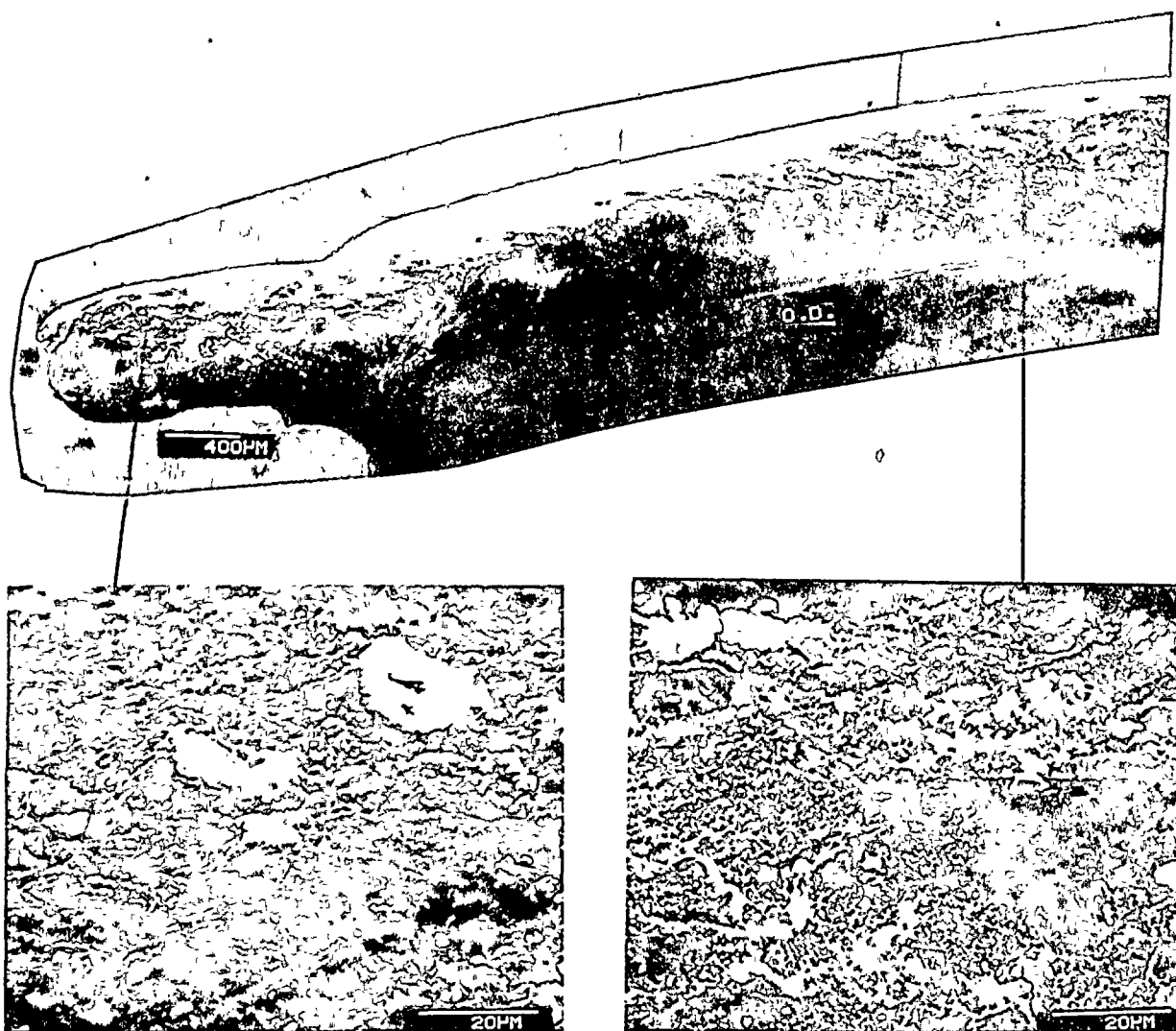


Fig. 4-9. SEM's of the fracture face at the bottom of the top portion of Tube R44-C55



Fig. 4-10. 180° view of ring at bottom of Tube R44-C54 (Top) and fractography on bottom fracture surface showing areas studied in more detail

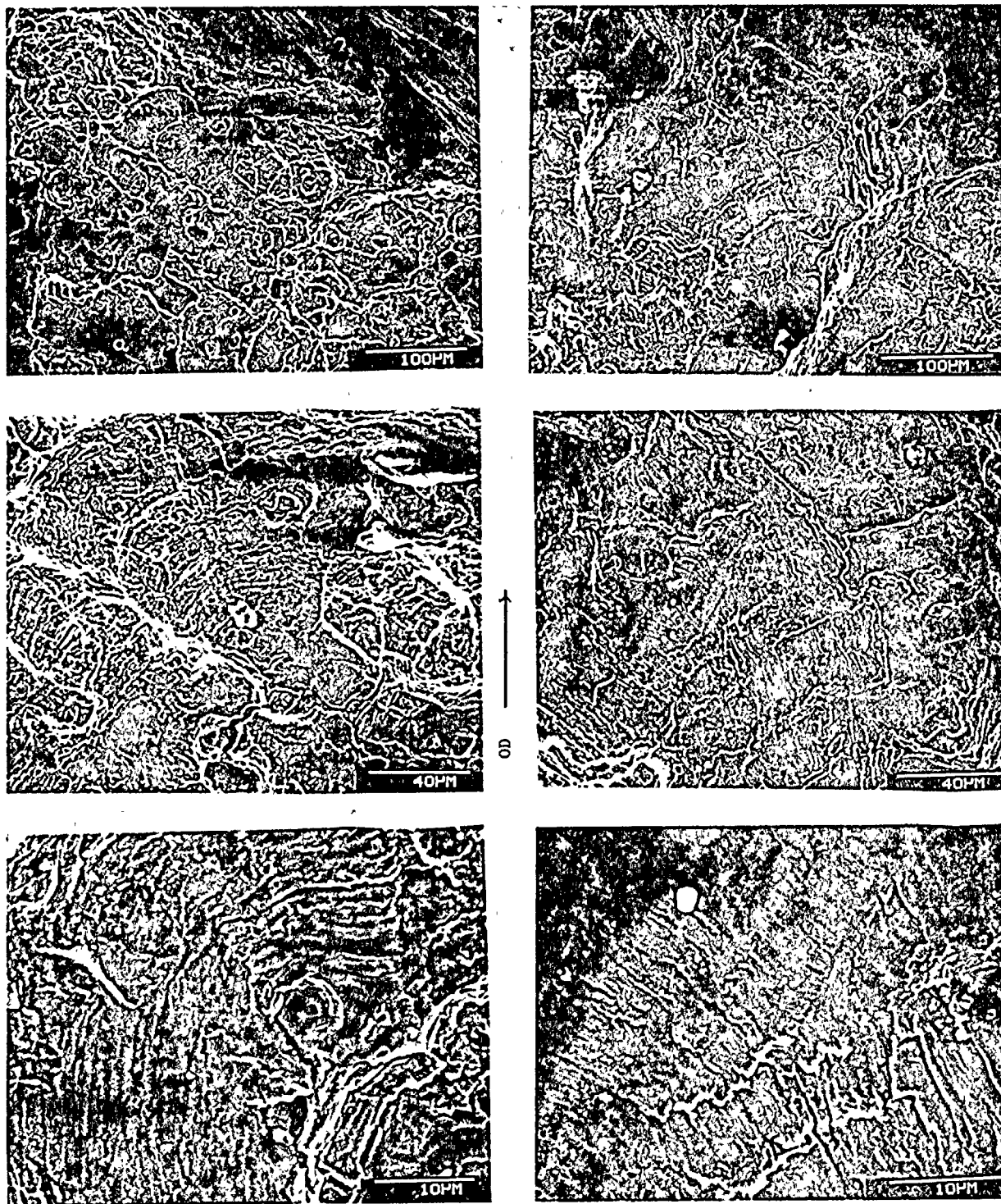
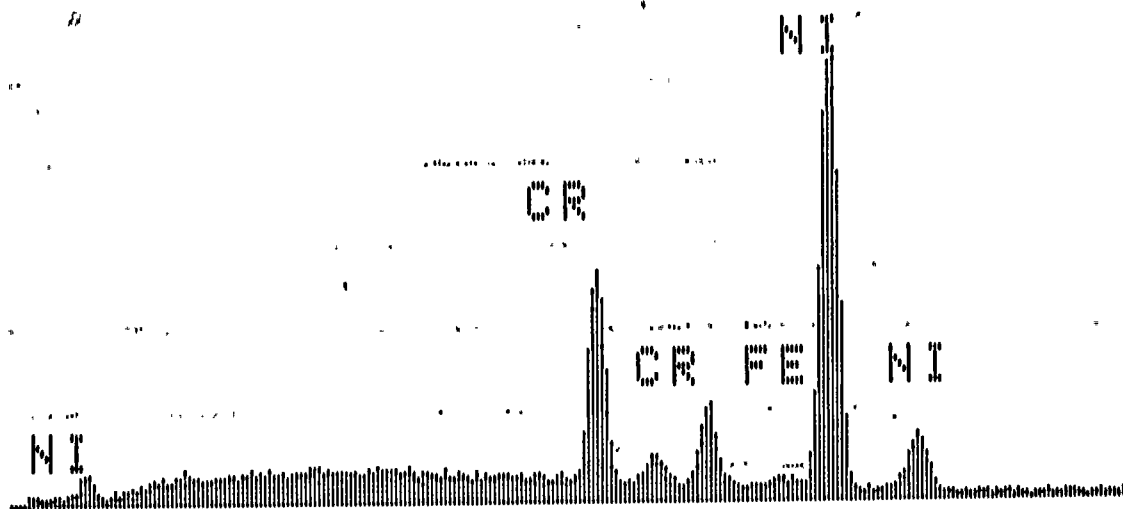


Fig. 4-11. Fractography on bottom fracture surface of Tube R44-C54;
Area 1 (left) and Area 2(right)



EDS Analysis		ASTM Spec.
Element	w/o	SB-163
& Line		w/o
Cr K α	17.0	14.0 to 17.0
Fe K α	8.5	6.0 to 10.0
Ni K α	74.4	72.0 (min)

Fig. 5-1. EDS spectrum and analysis for principal elements on Section 1A from Tube R44-C55
(Included are ASTM specifications).

Table 5-1

Mechanical Properties

Tube No.	Knoop Hardness (500 g)	R _B Hardness (1)	Yield Strength (0.2% offset) Ref. (2)	Ref (3)	Percent Elongation (4)
R44-C55	206.6	88	56,000	62,000	>28
R42-C55	171.3	80	45,000	45,000	>28

1) Converted by ASTM E140-79

2) Correlation establish on 24 tubes of Inconel 600 by R. G. Aspden

3) Estimated by correlations established in Inconel alloy 600, Hunting Alloy Products Division, the International Nickel Company, Inc.

4) No fissures developed when bent around a 3/32" dia. mandrel-calculated values.

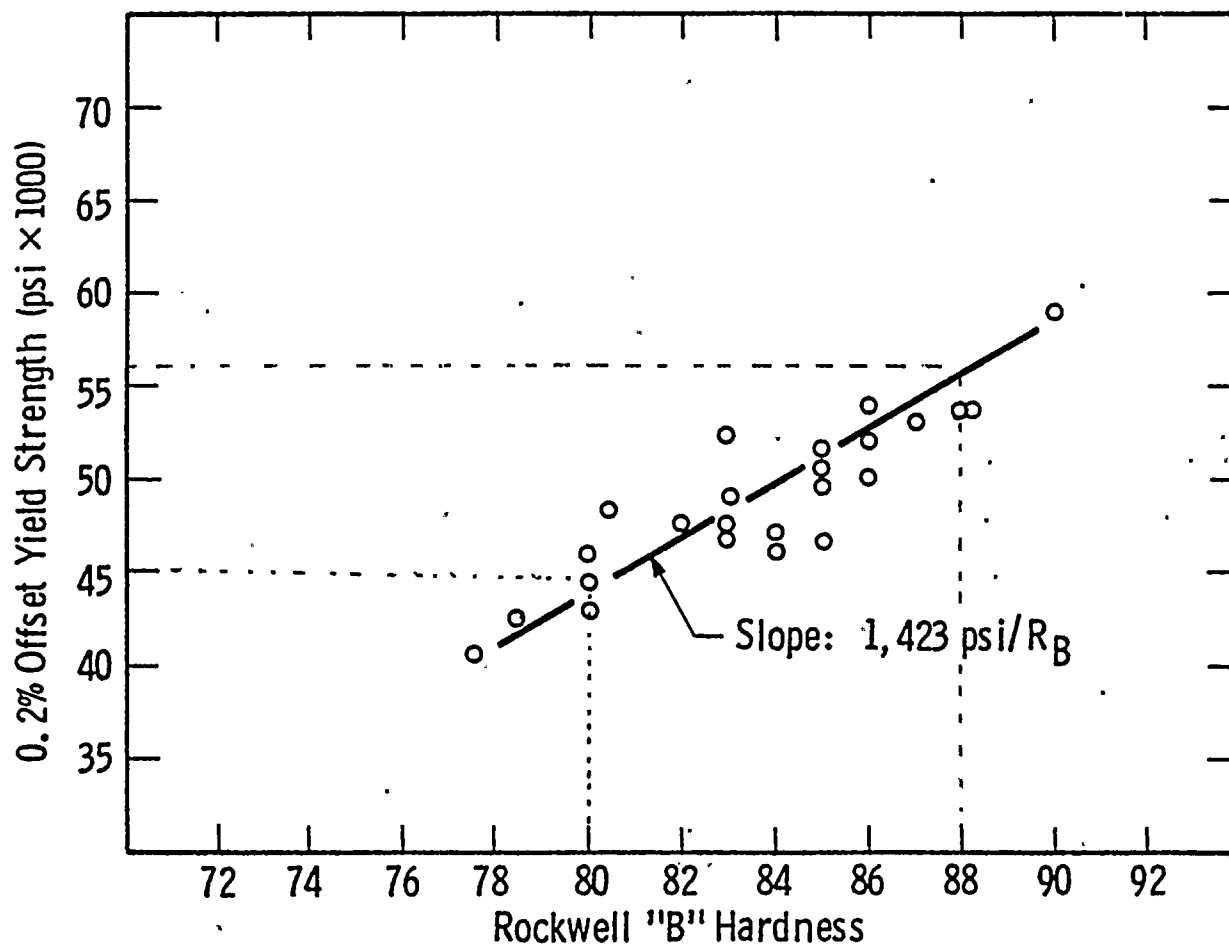


Fig. 5-2. Correlation of Rockwell "B" hardness and yield strength on 24 heats of Inconel 600 tubing and estimated strengths of two Ginna tubes (dashed lines).

